STADIUS
Center for Dynamical Systems, Signal Processing and Data Analytics

Citation/Reference	M. Lavanga et al., "Results of quantitative EEG analysis are associated with autism spectrum disorder and development abnormalities in infants with tuberous sclerosis complex," Submitt. to Comput. Methods Programs Biomed., pp. 1–28, 2020.
Archived version	Author manuscript: the content is identical to the content of the published paper, but without the final typesetting by the publisher
Published version	Submitted
Journal homepage	https://www.journals.elsevier.com/computer-methods-and-programs-in-biomedicine/
Author contact	your email mlavanga@esat.kuleuven.be your phone number +32 16 37 38 28
Abstract	Objective: The aim of this study is the investigation of early-life EEG background abnormalities or "dysmature" traits in infants with tuberous sclerosis complex (TSC) and their capacity to predict autism spectrum disorder or neurodevelopmental outcome. Methods: EEG data were prospectively collected from TSC patients during the EPISTOP trial (NCT02098759). Subjects were younger than 4 months, and ASD risk and neurodevelopmental outcome were assessed at the age of 2 years with the Autism Diagnostic Observation Scale 2 (ADOS-2) score and Bayley Scales of Infant and Toddler Development III (BSID-III). The EEG at the first visit was analyzed by means of Multiscale Entropy (MSE), multifractality (MFA), amplitude integrated EEG features and topological indices of the EEG network. These features were associated with both ASD and abnormal Bayley outcome of the infants using linear discriminant analysis. Results: The classification of the ASD patients shows that MFA and MSE had the best discrimination performances, with an area under the ROC curve AUC (MFA) = 0.74 and AUC(MSE) = 0.79 respectively, and kappa scores of Kappa(MFA) = 0.48 and Kappa(MSE) = 0.26. Concerning both abnormal Bayley outcome and ASD, the developmental abnormalities detection shows that entropy and fractal features outperform the other subsets of attributes and the multiclass analysis shows that those features can also discriminate patients with ASD from patients with only developmental abnormalities (Kappa(MFA) = 0.41 and Kappa(MSE) = 0.36).

Conclusion: Quantitative EEG analysis shows that a dysmature EEG, i.e. a signal with higher fractal regularity and lower entropy, is associated with autism spectrum disorder or abnormal Bayley outcome at 2 years of age. Significance: A quantitative analysis of the early-life EEG might provide a unique understanding of the brain functional processing for cognitive disorders or development disabilities, such as ASD, in TSC.

IR

(article begins on next page)

Computer Methods and Programs in Biomedicine

Results of quantitative EEG analysis are associated with autism spectrum disorder and development abnormalities in infants with tuberous sclerosis complex

--Manuscript Draft--

Manuscript Number:	
Article Type:	Full Length Article
Section/Category:	Biomedical signal and image processing methods
Keywords:	EEG, development, autism spectrum disorder, Bayley score, connectivity, multiscale entropy, mutlifractality
Corresponding Author:	Mario Lavanga, Biomedical Engineering KU Leuven: Katholieke Universiteit Leuven Leuven, Vlaams Brabant BELGIUM
First Author:	Mario Lavanga, Biomedical Engineering
Order of Authors:	Mario Lavanga, Biomedical Engineering
	Jessie De Ridder
	Katarzyna Kotulska
	Romina Moavero
	Paolo Curatolo
	Bernhard Weschke
	Kate Riney
	Martha Feucht
	Pavel Krsek
	Rima Nabbout
	Anna Jansen
	Konrad Wojdan
	Dorota Domanska-Pakiela
	Magdalena Kaczorowska - Frontczak
	Christoph Hertzberg
	Cyrille Ferrier
	Sharon Samueli
	Alena Jahodova
	Eleonora Aronica
	David Kwiatkowski
	Floor Jansen
	Sergiusz Jozwiak
	Lieven Lagae
	Alexander Caicedo
	Sabine Van Huffel
Manuscript Region of Origin:	Europe
Abstract:	Objective: The aim of this study is the investigation of early-life EEG background abnormalities or “dysmature” traits in infants with tuberous sclerosis complex (TSC)

Powered by Editorial Manager® and ProduXion Manager® from Aries Systems Corporation

	and their capacity to predict autism spectrum disorder or neurodevelopmental outcome. Methods: EEG data were prospectively collected from TSC patients during the EPISTOP trial (NCT02098759). Subjects were younger than 4 months, and ASD risk and neurodevelopmental outcome were assessed at the age of 2 years with the Autism Diagnostic Observation Scale 2 (ADOS-2) score and Bayley Scales of Infant and Toddler Development III (BSID-III). The EEG at the first visit was analyzed by means of Multiscale Entropy (MSE), multifractality (MFA), amplitude integrated EEG features and topological indices of the EEG network. These features were associated with both ASD and abnormal Bayley outcome of the infants using linear discriminant analysis. Results: The classification of the ASD patients shows that MFA and MSE had the best discrimination performances, with an area under the ROC curve AUC (MFA) = 0.74 and AUC(MSE) = 0.79 respectively, and kappa scores of Kappa(MFA) = 0.48 and Kappa(MSE) = 0.26. Concerning both abnormal Bayley outcome and ASD, the developmental abnormalities detection shows that entropy and fractal features outperform the other subsets of attributes and the multiclass analysis shows that those features can also discriminate patients with ASD from patients with only developmental abnormalities (Kappa(MFA) = 0.41 and Kappa(MSE) = 0.36). Conclusion: Quantitative EEG analysis shows that a dysmature EEG, i.e. a signal with higher fractal regularity and lower entropy, is associated with autism spectrum disorder or abnormal Bayley outcome at 2 years of age. Significance: A quantitative analysis of the early-life EEG might provide a unique understanding of the brain functional processing for cognitive disorders or development disabilities, such as ASD, in TSC.
Suggested Reviewers:	Jurriaan M Peters Assistant Professor of Neurology, Harvard Medical School, Boston Childrens Hospital: Boston Children's Hospital juriaan.peters@childrens.harvard.edu Great expertise in connectivity, autism and TSC
	Lucia Billeci University of Pisa lucia.billeci@centropiaggio.unipi.it Great expertise in connectivity and autism
Opposed Reviewers:	

Dear Editor-in-chief

I am Mario Lavanga, corresponding author of the article “Results of quantitative EEG analysis are associated with autism spectrum disorder and development abnormalities in infants with tuberous sclerosis complex”, and I am writing to you to submit my manuscript for consideration as a research paper. The main goal of the study was the prediction of future development abnormalities of young infants based on the EEG monitoring in the first months of life. The current study is an extensive investigation of a variety of quantitative EEG methods to associate EEG abnormalities with future development abnormalities in 61 patients with Tuberous Sclerosis Complex.

Tuberous Sclerosis Complex (TSC) is a multisystems genetic disorder which leads to autism spectrum disorder (ASD) in 40% of the cases. Clinicians are interested in the automatic analysis of EEG in the first weeks of life of TSC patients for three main reasons. Firstly, they want to diagnose the condition of ASD based on EEG waveforms. Secondly, they are interested to detect abnormal cognitive or motor outcome in terms of Bayley score. Thirdly, clinicians look for methods to discriminate the condition of autism from generic abnormal cognitive skills. The current analysis is an investigation based on state-of-the-art methods to address all those questions with both univariate and multivariate analysis. All the methodologies were compared to show which the most pivotal information to extract from the EEG associated with development delays or abnormalities. The main novelty of this analysis does not only lie in the extreme young age of the study population (on average, the data were collected in the first month of life), but also on two main methodological aspects. The study applied a comparison of both connectivity and nonlinear methods to assess which could perform best in clinical practice. Interestingly, the results show that a higher Hurst regularity and lower complexity are the most performative features, which are also associated with an EEG with lower maturity. On top of that, the study is the first one to perform an automatic assessment of the best threshold to define for development delays in terms of Bayley score.

Our findings fit a potential publication in Computer Methods and Programs in Biomedicine. The current analysis reports a first comparison of a variety of quantitative EEG methods to detect autism and developmental delay. Furthermore, it provides a new quantitative EEG application in an extreme young population. Finally, it looks to provide a mathematical definition to the concept of development delay and its relationship with EEG dysmaturity. The complexity of the clinical problem and the comparison of multiple methods and computer strategies required an extended manuscript, which goes beyond the suggested limit of 3500 words. However, we are confident in the interest of the scientific community of CMPB to provide a new frontiers in early-life EEG analysis and prediction of development problems.

Results of quantitative EEG analysis are associated with autism spectrum disorder and development abnormalities in infants with tuberous sclerosis complex

Mario Lavanga[1], Jessie De Ridder[2], Katarzyna Kotulska[3], Romina Moavero[4,5], Paolo Curatolo[4], Bernhard Weschke[6], Kate Riney[7,8], Martha Feucht[9], Pavel Krsek[10], Rima Nabbout[11], Anna C. Jansen[12], Konrad Wojdan[13,14], Dorota Domanska-Pakieła[3], Magdalena Kaczorowska-Frontczak[3], Christoph Hertzberg[15], Cyrille H. Ferrier[16], Sharon Samueli[9], Alena Jahodova[10], Eleonora Aronica[17], David J. Kwiatkowski[19], Floor E. Jansen[16], Sergiusz Jóźwiak[3,20], Lieven Lagae[2], Sabine Van Huffel[1], Alexander Caicedo[21] on behalf of the EPISTOP consortium

Highlights

1. The early-life EEG of a TSC patients with autism spectrum disorder might be a dysmature EEG, defined as signal with higher discontinuity, slow-wave persistence and asynchrony
2. A dysmature EEG has the following quantitative traits: lower entropy, higher fractal regularity and higher EEG network resilience
3. The dysmature or background EEG abnormalities can also discriminate ASD from other developmental abnormalities
4. Early-life quantitative EEG analysis in young infants with TSC can detect and diagnose later developmental disabilities

Manuscript File Click here to view linked References

Results of quantitative EEG analysis are associated with autism spectrum disorder and development abnormalities in infants with tuberous sclerosis complex

Mario Lavanga[1], Jessie De Ridder[2], Katarzyna Kotulska[3], Romina Moavero[4,5], Paolo Curatolo[4], Bernhard Weschke[6], Kate Riney[7,8], Martha Feucht[9], Pavel Krsek[10], Rima Nabbout[11], Anna C. Jansen[12], Konrad Wojdan[13,14], Dorota Domanska-Pakieła[3], Magdalena Kaczorowska-Frontczak[3], Christoph Hertzberg[15], Cyrille H. Ferrier[16], Sharon Samueli[9], Alena Jahodova[10], Eleonora Aronica[17], David J. Kwiatkowski[19], Floor E. Jansen[16], Sergiusz Jóźwiak[3,20], Lieven Lagae[2], Sabine Van Huffel[1], Alexander Caicedo[21] on behalf of the EPISTOP consortium

1 Department of Electrical Engineering (ESAT), STADIUS Centre for Dynamical Systems, Signal Processing and Data Analytics, KU Leuven, Leuven Belgium

2 Department of Development and Regeneration, Section Pediatric Neurology, University of LeuvenKU Leuven, Leuven, Belgium

3 Department of Neurology and Epileptology, The Children's Memorial Health Institute, Warsaw,Poland

4 Child Neurology and Psychiatry Unit, Systems Medicine Department, Tor Vergata University, Rome, Italy

5 Child Neurology Unit, Neuroscience and Neurorehabilitation Department, “Bambino Gesù”, Children’s Hospital, Rome, Italy

6 Department of Child Neurology, Charité University Medicine Berlin, Berlin, Germany

7 Neuroscience Unit, Queensland Children’s Hospital, Brisbane, Australia

8 University of Queensland School of Medicine, Brisbane, Australia

9 Department of Pediatrics, Medical University Vienna, Vienna, Austria

10 Department of Paediatric Neurology, Charles University, Second Faculty of Medicine, Motol University Hospital, Prague, Czech Republic

11 Department of Pediatric Neurology, Reference Centre for Rare Epilepsies, Necker- Enfants Malades Hospital, University Paris Descartes, Imagine Institute, Paris, France

12 Pediatric Neurology Unit - UZ Brussel, Brussels, Belgium

13 Transition Technologies, Warsaw, Poland

14 Warsaw University and Technology, Institute of Heat Engineering, Warsaw, Poland

15 Diagnose und Behandlungszentrum für Kinder und Jugendliche, Vivantes Klinikum Neukölln, Berlin, Germany

16 Department of Child Neurology, Brain Centre, University Medical Centre Utrecht, The Netherlands

17 Amsterdam UMC, University of Amsterdam, Department of (Neuro)Pathology, Amsterdam, The Netherlands

18 Stichting Epilepsie Instellingen Nederland (SEIN), The Netherlands

19 Brigham and Women's Hospital, Harvard Medical School, Boston, USA

20 Department of Child Neurology, Medical University of Warsaw, Warsaw, Poland

21 Applied Mathematics and Computer Science, School of Engineering, Science and Technology, Universidad del Rosario, Bogotá, Colombia

Highlights

1. The early-life EEG of a TSC patients with autism spectrum disorder might be a dysmature EEG, defined as signal with higher discontinuity, slow-wave persistence and asynchrony
2. A dysmature EEG has the following quantitative traits: lower entropy, higher fractal regularity and higher EEG network resilience
3. The dysmature or background EEG abnormalities can also discriminate ASD from other developmental abnormalities
4. Early-life quantitative EEG analysis in young infants with TSC can detect and diagnose later developmental disabilities

Structured Abstract

Objective: The aim of this study is the investigation of early-life EEG background abnormalities or "dysmature" traits in infants with tuberous sclerosis complex (TSC) and their capacity to predict autism spectrum disorder or neurodevelopmental outcome.

Methods: EEG data were prospectively collected from TSC patients during the EPISTOP trial (NCT02098759). Subjects were younger than 4 months, and ASD risk and neurodevelopmental outcome were assessed at the age of 2 years with the Autism Diagnostic Observation Scale 2 (ADOS-2) score and Bayley Scales of Infant and Toddler Development III (BSID-III). The EEG at the first visit was analyzed by means of *Multiscale Entropy (MSE),* multifractality (MFA), amplitude integrated EEG features and topological indices of the EEG network. These features were associated with both ASD and abnormal Bayley outcome of the infants using linear discriminant analysis.

Results: The classification of the ASD patients shows that MFA and MSE had the best discrimination performances, with an area under the ROC curve AUC (MFA) = 0.74 and AUC(MSE) = 0.79 respectively, and kappa scores of Kappa(MFA) = 0.48 and Kappa(MSE) = 0.26. Concerning both abnormal Bayley outcome and ASD, the developmental abnormalities detection shows that entropy and fractal features outperform the other subsets of attributes and the multiclass analysis shows that those features can also discriminate patients with ASD from patients with only developmental abnormalities (Kappa(MFA) = 0.41 and Kappa(MSE) = 0.36).

Conclusion: Quantitative EEG analysis shows that a dysmature EEG, i.e. a signal with higher fractal regularity and lower entropy, is associated with autism spectrum disorder or abnormal Bayley outcome at 2 years of age.

Significance: A quantitative analysis of the early-life EEG might provide a unique understanding of the brain functional processing for cognitive disorders or development disabilities, such as ASD, in TSC.

1. Introduction

Quantitative and automatic EEG analysis has been proven useful for early detection of autism spectrum disorder (ASD) (Billeci et al., 2013)(Peters et al., 2013). An extensive review has recently shown which EEG features can be computed to possibly detect ASD, both at rest or during specific tasks (Billeci et al., 2013). Namely, multiscale entropy (MSE), signal fractality and EEG connectivity have been the subject of multiple studies to investigate ASD risk. By computing the MSE, Bosl et al. obtained a lower EEG entropy in infants at high risk of ASD and a detection accuracy of 70% at age 6 months (Bosl, Tierney, Tager-Flusberg, & Nelson, 2011). Peters et al. (Peters et al., 2013) found EEG networks with higher resilience in case of ASD, where resilience was defined as a capacity to resist a failure in the network and it is measured as the reduction of global efficiency, after the removal of a node or edge (Peters et al., 2013; Rubinov & Sporns, 2010a).

However, current EEG studies on ASD do not focus on patients below 6 months or close to birth (Peters et al., 2013) (Bosl et al., 2011) (Billeci et al., 2013), although such early-stage analysis could be beneficial for patients. Especially, patients who are diagnosed with genetic disorders such as Tuberous Sclerosis Complex (TSC) may present a variety of different outcomes. Tuberous Sclerosis Complex (TSC) is a multisystem and autosomal dominant and a number of studies have shown that the majority of infants with TSC develop epilepsy and a variety of neurodevelopment abnormalities including intellectual disability and autism spectrum disorder (ASD) (Curatolo, 2015). However, studies with a specific focus on quantitative analysis of early-life EEG and TSC–associated Pervasive Developmental Disorders (PDD), especially ASD, were not published.

Research of EEG background abnormalities in premature infants and neonates showed that a dysmature EEG was associated with a poor cognitive outcome (Biagioni, Bartalena, Biver, Pieri, & Cioni, 1996; Le Bihannic, Beauvais, Busnel, de Barace, & Furby, 2012; Okumura, Hayakawa, Kato, Watanabe, & Kuno, 2002; D. Selton, Andre, Debruille, Deforge, & Hascoët, 2013; Daniele Selton et al., 2010) . Pavlidis et al. (Pavlidis, Lloyd, & Boylan, 2017) and Watanabe et al. (Watanabe, Hayakawa, & Okumura, 1999) defined the main traits of a disorganized or dysmature EEG in preterm infants with a poor clinical or developmental outcome as discontinuity, persistence of slow-waves, asynchrony or lagged asynchrony among bursts.

Multiple studies quantified the presence of dysmature EEG in premature infants as a type of background characterized by a lower entropy, higher regularity and higher EEG connectivity (De Wel et al., 2017; M. Lavanga, De Wel, Caicedo, Jansen, et al., 2017; Mario Lavanga et al., 2018; John M. O'Toole, Pavlidis, Korotchikova, Boylan, & Stevenson, 2019; Zhang et al., 2009). The state of the art clearly suggests that both the autistic EEG and preterm dysmature EEG presents the same attributes in term of entropy, regularity and connectivity, but a complete overview of all those features was never investigated in young infants at risk of developmental disabilities.

The aim of this study was the assessment of the relationship between quantitative early-EEG characteristics, neurodevelopment and ASD in a cohort of infants with TSC. Based on the infants' data in the first months of life, we analyzed electrophysiological data to automatically predict ASD diagnosis and abnormal neurodevelopment. Additionally, we investigated the relationship between early-life EEG and cognitive, motor and language Bayley score.

2. Material and methods

2.1 Patient sample

This EEG study was part of the EPISTOP project, which is a multicentre and prospective study to assess biomarkers of epileptogenesis in tuberous sclerosis complex (NCT02098759) and to analyze whether preventive treatment before seizure onset could improve epilepsy and neurodevelopmental outcome in TSC children at two years of age. Patients with a definite diagnosis of TSC and age ≤ four months were enrolled from November 2013 to August 2016 at 10 different sites, after the approval of local ethical committees. Informed consent was obtained from caregivers in accordance with the Declaration of Helsinki.

The final number of patients involved in this EEG study was 61. The gestational age (age at birth) of the included patients had a range from 29.71 weeks until 42 weeks. The median GA was 38.14 weeks, as shown in Table 1.

2.2 EEG recordings

Patients had serial video EEG recordings, but this study focused only on the first-EEG, recorded at four weeks after patients' enrollment. The EEG was recorded according to the 10-20 system for at least one hour. The minimum sample rate was 128 Hz and the electrode impedance was below 5 kOhm. Normally, a set of 19 electrodes was used, but a reduced array with nine electrodes was allowed in infants below 3 months corrected age ($F_{p1}, F_{p2}, C_3, C_4, T_4, T_3, O_1, O_2, C_z$). The quantitative analysis focused only on this set of electrodes and Cz was used as reference channel (which was then excluded from further processing). The median EEG recording time was 73.42 min (around 1 h 13 min) and the median age at the moment of the recording was 42.57 weeks (around 1 month and 1 week from birth) for the entire pool of recordings. The age at the moment of recording had a range from 35.86 weeks to 57 weeks.

2.3 Neuropsychological assessment

In order to assess the relationship between neurodevelopmental outcome and EEG abnormalities, we used the following scales to define developmental outcomes. First, the Autism Diagnostic Observation Scale 2 (ADOS-2) score or Diagnostic and Statistical Manual of Mental Disorders-5 (DSM-5) were used as clinical criteria to evaluate the presence of ASD at 24 months. (Moavero et al., 2019). Second, the Bayley Scales of Infant and Toddler Development III (BSID-III) were used to evaluate the cognitive developmental quotient (DQ), language DQ and motor DQ at two years of age. The median Cognitive DQ was 75, the median language DQ was 68 and the median motor DQ was 73 for the entire dataset.

An overview of the patients' demographics is reported in Table 1 for all the EEG recordings and two groups: patient who had ASD diagnosis (ASD) and those who did not have an ASD diagnosis (NO ASD). The table reports the median gestational age (GA or age at birth) , the median age at the time of the recording in weeks for two groups and the median BSID-III scores at 2 years. We also reported the total number of ASD diagnoses and TSC mutations caused by the gene *TSC2* in the patients' cohort. Figure 2 shows two examples of EEG traces from an ASD patient and from a patient without ASD.

Table 1. Summary of patient data set: GA (gestational age or age at birth), PMA (postmenstrual age or chronological at time of the recording) and development quotients at 2 years of age based on Bayley Scales of Infant and Toddler Development III (BSID-III): cognitive, language and motor scores. The first column reports the demographics of the entire pool of EEG recordings, while the data are split for ASD (Autism Spectrum Disorder) and NO ASD outcomes at 2 years of age in other two columns. Statistics are reported as median [IQR]. The last row represents the number of tuberous sclerosis complex mutations caused by the gene *TSC2* in the two groups.

	EEG (n= 61)	**ASD (n=19)**	**NO ASD (n=42)**
GA(weeks)	38.14 [37-40]	38.43 [37-40]	38 [37-40]
Age at Recording(weeks)	42.57 [40.36-45.68]	41.57 [39.11-43.43]	43.14 [40.86-46.43]
EEG(min)	73.42 [56.95-93.92]	82.08 [60.47-109.1]	71.04 [55-88.5]
BSID-III Cognitive	75 [65-90.25]	65 [55-80]	82.5 [70-95]
BSID-III Language	68 [61.25-78.25]	62 [50.75-66.5]	71 [65-94]
BSID-III Motor	73 [67-85]	67 [55.75-72.25]	77.5 [70-92]
TSC2	44/61	14/19	30/42

Table 2 – Overview of the univariate and multivariate features derived from the physiological signal in the study divided in 5 categories: power, multiscale entropy, multifractality, connectivity features derived by the mean squared coherence (MSC) and connectivity features derived by the imaginary coherence. For the univariate feature groups (first three rows), each attribute was derived for each channel (as indicated by the third column). For the spectral features and the connectivity features, each attribute was derived for the main EEG frequency bands (as indicated by the second column). The last column represents the number of features extracted for each category. CI stands for complexity index, MSE(3) and MSE(20) is SampEn at scale 3 and at scale 20 and ΔH stands for the difference between the minimal and maximal Hurst exponents. Nsup is the number of superfluous connections, Clust is the average clustering coefficient, PL is the path length and Ratio is the average between long-range and short-range connections.

Features	**Frequency bands**	**Channels**	**Properties**	**Number**
Power	$\delta_1, \delta_2, \theta, \alpha, \beta$	$F_{p1}, F_{p2}, C_3, C_4, T_4, T_3, O_1, O_2$	Band power	40
MSE		$F_{p1}, F_{p2}, C_3, C_4, T_4, T_3, O_1, O_2$	CI, MSE(3), MSE(20), sampen(2), sampen(3)	40
Multifractality		$F_{p1}, F_{p2}, C_3, C_4, T_4, T_3, O_1, O_2$	HurstExp, c2,c3, ΔH	32
MSE - Connectivity	$\delta_1, \delta_2, \theta, \alpha, \beta$		PL, Ratio - PL/GE, Clust, Nsup	20
ImCoh - Connectivity	$\delta_1, \delta_2, \theta, \alpha, \beta$		PL, Ratio - PL/GE, Clust, Nsup	20

Table 3. Overview of the NEURAL Features obtained with the toolbox described in (Toole et al., 2017), where the reader can find more details. Spectral and rEEG features were computed for the main EEG frequency bands (as reported by the second column). max IBI – maximum interburst interval. The last column indicates the number of features extracted for each category.

NEURAL Features	**Frequency bands**	**Properties**	**Number**
Amplitude		Mean, standard deviation, skewness, kurtosis, Envelope mean, Envelope standard deviation	25
Spectral	$\delta, \theta, \alpha, \beta$	Band power, relative power, entropy, edge frequency, spectral flatness, spectral difference (Diff)	21
Range EEG (rEEG)	$\delta, \theta, \alpha, \beta$	Mean, median, lower margin, upper margin, width, standard deviation, coefficient of variation, asymmetry	32
Burst		Burst percentage, median and max IBI, number of bursts	4

2.4 Quantitative EEG analysis

The quantitative EEG analysis was based on the extraction of features that are associated to the most important traits of dysmature EEG, which are discontinuity, persistence of slow waves and asynchrony (Pavlidis et al., 2017). After EEG preprocessing, the computed features were combined in different classification and regression models to determine the development abnormalities of the patient, as displayed in Figure 1. A summary of all attributes is reported in Table 2 and Table 3. The quantitative EEG analysis was performed with available MATLAB subroutines or toolboxes which are available online.

2.4.1 EEG preprocessing

EEG data were band-pass filtered between [0.5-32] Hz (FIR filter, with limited ripple and 40 db attenuation) and resampled at 64 Hz. Each channel was split in non-overlapping windows of different length based on the computed feature and each window was kept in the processing if the following criteria were met: standard deviation below 50 μV, absolute difference sample-to-sample below 50 μV and absolute amplitude below 200 μV (Isler, Stark, Grieve, Welch, & Myers, 2018). If one of the channel did not meet all the reported criteria, it was excluded from further analysis. If more than 50% of channel did not meet all the reported criteria, the entire window was excluded from further processing.

2.4.2 Power analysis

The power spectral density (PSD) was estimated in 30 s window with the non-parametric Welch approach. The length of the subwindow was 4s with 70% overlap. The power was computed in the following frequency bands $\delta_1 = (0.5 - 2]\ Hz,\ \delta_2 = (2 - 4]\ Hz, \theta = (4 - 8]\ Hz, \alpha = (8 - 16]\ Hz$, $\beta = (16 - 32]\ Hz$ and log-transformed. The power features were grand-averaged for each recording along the window dimension. The split of the delta band in δ_1 and δ_2 is explained by the shift in the spectral edge frequency and the power distribution of the EEG during maturation (Wallois, 2010).

2.4.3. Entropy features

Based on the recent findings by (Costa, Goldberger, & Peng, 2002; De Wel et al., 2017; Kaffashi, Scher, Ludington-Hoe, & Loparo, 2013; Lake & Moorman, 2011; Zhang et al., 2009), the traits of EEG discontinuity and slow-wave persistence can be measured by means of Sample Entropy (SampEn) and the multiscale entropy (MSE). The former measures how predictable the signal is by counting how many templates of size m match within a certain tolerance r, while the multiscale entropy measures SampEn at the different scales τ. The tolerance r is defined as 20% the standard deviation of the signal (Lake & Moorman, 2011) and the scale τ represents the length of the windows of the coarse-graining process of the signal (Costa et al., 2002).

Following the pioneering studies of (De Wel et al., 2017; Zhang et al., 2009), the main features derived in this study to describe the dysmaturity patterns were:

- SampEn with embedding dimension $m = 2$ and $m = 3$
- The MSE at scale 3 and 20, i.e. $MSE(\tau = 3)$ and $MSE(\tau = 20)$
- The complexity index $CI = \sum_\tau MSE(\tau)$, which is the area under the MSE curve

The SampEn and $MSE(\tau = 3)$ represent the information at small scales or high frequency, while $MSE(\tau = 20)$ represents the information at longer scales or lower frequency (Hoyer et al., 2013). The latter is fundamental to show the effect of the persistence of slow-waves, while CI is a general measure of overall irregularity or entropy. All features were estimated in non-overlapping 150s windows and grand-averaged for each recording.

2.4.5 Fractality features

The discontinuity and the slow-wave persistence can also determine an EEG time-series with a power-law PSD (known also as 1/f spectrum), which is typical of a fractal or scale-free signals (Kesić & Spasić, 2016; Lavanga et al., 2017; Popivanov et al., 2006)(John M. O'Toole et al., 2019). The rate of decay is normally controlled by one or more Hurst Exponents in case of multifractal signals, such as a discontinuous EEG (Wendt, Abry, & Jaffard, 2007) (M Lavanga et al., 2017). The distribution of Hurst exponents, known as singularity spectrum (SS), is normally computed via wavelet transform (Jaffard, Lashermes, & Abry, 2006) and can be used to describe the dysmature EEG with the following set of parameters:

- The main Hurst exponent (HurstExp) at the location of the SS maximum, which represents the main regularity in the signal
- The parameters c_2 and c_3, which respectively represent the width and the asymmetry of SS and measure the "amount of fractals" inside the time series.

- The difference between maximal and minimal Hurst exponents ΔH of the SS, which resembles c_2 and assesses the number of singularities in a signal. The higher the number of singularities, the higher the discontinuity.

These features were computed in non-overlapping 150s windows and by means of the WLBFM toolbox (Wendt et al., 2007). Subsequently, they were grand-averaged for each recording.

2.4.6. NEURAL features

The dysmaturity of EEG was also quantified by means of the NEURAL toolbox (available on GitHub) (O'Toole & Boylan, 2017), which estimates an exhaustive range of features that can be obtained by amplitude, burst and spectral information, connectivity analysis and the range EEG (rEEG). The latter represents an estimation of the amplitude integrated EEG (aEEG) (O'Toole & Boylan, 2017). It is important to mention that rEEG was used to quantify the level of dysmaturity, by means of its lower and upper margin and the rEEG asymmetry, defined as proximity of the median towards one of the two margins, based on the studies of (Hellström-Westas, 2006). Besides the rEEG features, the NEURAL toolbox computes statistics of the EEG amplitudes, the power in the different frequency bands and the spectral difference, the burst percentage and the time interval between bursts. The complete list of features is reported in (O'Toole & Boylan, 2017) and in Table 3. NEURAL features were computed in 2 secs for spectral features with 50% overlap, 2 secs for amplitude features without overlap and 4 secs for connectivity features with 75% overlap. As already mentioned, the NEURAL attributes were grand-averaged for each recording.

2.4.7. EEG connectivity

Functional cortical connectivity was analysed by means of Imaginary Coherence (IC) and Magnitude Squared Coherence (MSC), which are both derived from the coherence $C_{xy}(f) = \frac{P_{xy}(f)}{\sqrt{P_{xx}(f)P_{yy}(f)}}$. This index is the ratio between $P_{xy}(f)$, the cross-spectrum between two channels x and y and the square root of the product of two autospectra P_{xx}, P_{yy}. MSC is then defined as the squared magnitude of the coherency, i.e. $k_{xy}^2(f) = |C_{xy}(f)|^2$, while IC is the imaginary part of the coherency, i.e. $I_{xy}(f) = |\Im\left(C_{xy}(f)\right)|$. The latter represents the lagged connectivity, while the former is the instantaneous connectivity.

The statistical validity of each coupling was then tested with *amplitude adjusted Fourier transform (AAFT)* surrogates, with a level of statistical significance $\alpha = 0.05$ (González et al., 2011). Therefore, 19 surrogates were used to generate a threshold $T(f)$ in function of the frequency for both $k_{xy}^2(f)$ and $I_{xy}(f)$. The actual MSC coupling was then represented by the average of $k_{xy}^2(f)$ in the following frequency bands δ_1, δ_2, θ, α and β. In case of IC, the maximal amplitude of $|\Im\left(C_{xy}(f)\right)|$ was then considered in the same frequency bands (Nolte et al., 2004). The EEG connectivity coherency was estimated using a Welch-periodogram approach for non-overlapping 30 s windows, with 70% overlap and 4s subwindows (Bortel & Sovka, 2007; González et al., 2011).

2.4.8. Graph Theory

Functional connectivity methods such as IC and MSC generate EEG undirected networks: the nodes represent the EEG channels and the weighted edges represent the intensity of the coupling between channels (Bullmore & Sporns, 2009). Graphs can be characterized by different topological measures

(Rubinov & Sporns, 2010b). The most common measure of integration is the path length (PL), which is the average length of the shortest paths among nodes in the network. The global efficiency (GE) is the average of all inverse path lengths. The PL is normally driven by weaker connections (or longer distances) in the graph, while the GE is driven by the strongest connections (or shortest distances) (Peters et al., 2013). Therefore, one can measure the long-range over short-range connections ratio as the ratio between PL and GE. Another common index is the clustering coefficient, which represents the likelihood of two nodes to be connected to a third one. In order to give a representative metric of clustering node, one can compute the average clustering coefficient. An overview of the different topological indices is reported in Table 2. The topological indices were computed by means of the Brain Connectivity toolbox (Rubinov & Sporns, 2010b).

Recently, Peters et al. investigated the resilience of EEG networks, which is defined as the ability to resist random or target attacks (removal of edges or nodes) and keep the global efficiency close to the original one (Peters et al., 2013). In this study, the resilience has been derived as the number of superfluous connections, which are the connections that can be removed without significant changes in the EEG network. The details of this methodology are reported in Appendix A.

2.5 ASD and development outcome prediction

The pipeline followed for the quantitative EEG analysis was as follows: first the EEG channels were preprocessed in order to remove artifacts and to improve the quality of the signals. Second, EEG features were extracted in order to quantify dysmaturity. Finally, the dysmaturity features were related to the neurodevelopmental outcome of the infant. In order to meet the four stated objectives and investigate the relationship between EEG abnormalities and developmental abnormalities in TSC infants (at two years of age), four different strategies were pursued, as reported in table 4 and Figure 1.

2.5.1 *Automatic classification of ASD patients*

The first strategy aimed to design a classifier to predict an ASD outcome at 2 years with EEG dysmaturity features. A set of 5 features was selected for a binary classification scheme, whose target variable was represented by autism diagnosis (ASD vs NO ASD).The features selection was based on the highest ratio between higher inter-group variance and lower intra-group variance (Chen & Lin, 2006) for each feature group (power, fractality, entropy, NEURAL, connectivity) and for the entire pool of attributes. We selected 5 features in order to guarantee that the number of predictors is below 10% of the total number of patients (Floyd & Warmuth, 1995). A classifier was implemented with a Linear discriminant analysis (LDA) algorithm with 3-fold testing: the algorithm was iterated 3 times and the classifier was first trained on 2/3 of data as training set and tested on the remaining 1/3. LDA hyperparameters were tuned using 10-fold cross-validation (9/10 of the training set is used for training set and 1/10 is used as validation set). The classification results were reported as classification error, area under the receiver operating characteristic (ROC) curve (AUC, defined as measure of classification accuracy) and Cohen's kappa score (Table 4). Cohen's Kappa is a statistical measure of the agreement between machine labels and true labels and it corrects for the agreement expected by chance. Cohen's Kappa is usually defined as

$$k = \frac{p_o - p_e}{1 - p_e},$$

where p_o represents the observed agreement and p_e denotes the expected agreement. The Cohen's kappa is usually a more suitable index for imbalanced datasets. Additionally, the statistical differences

among features represented by autism diagnosis (ASD vs No-ASD) were tested with a Kruskal-Wallis test for each separate channel.

2.5.2 *Automatic classification of abnormal outcomes*

The second strategy aimed to predict an abnormal developmental outcome at 2 years. Therefore, it consisted of a binary classification of patients based on EEG dysmaturity features with a slight modification of the target variable compared to the first strategy. The positive class or abnormal outcome was represented by either the ASD diagnosis, an abnormal Bayley score or both. An abnormal Bayley score was here defined as one or more of the three BSID-III scores at 2 years below a certain threshold. Consequently, this strategy tries to include any possible abnormality (abnormal vs normal), whether it is a developmental disorder like ASD, or a global or specific developmental impairment (e.g. low motor DQ, low cognitive DQ). The definition of abnormal development outcome with Bayley score is linked to the threshold. The clinical cut-off is usually 70 or 80 since these are associated with a lower mental and cognitive outcome (Johnson, Moore, & Marlow, 2014). However, the literature does not show a clear consensus on which threshold has to be applied to define developmental delay (Duncan et al., 2015; Johnson et al., 2014). Therefore, multiple thresholds were investigated to define the positive class in the range from 55 to 80 with steps of width 3, i.e. [55:3:80]. The threshold 55 represents the minimum Bayley score in the dataset, while 80 is one of the highest thresholds in the literature to define developmental delay (Duncan et al., 2015; Johnson et al., 2014). The classifier was designed based on the same LDA algorithm used for ASD detection. The classification results were reported as AUC and Cohen's kappa score in function of the threshold.

2.5.3 Multiclass analysis of abnormal Bayley outcomes, ASD and normal patients

The third strategy is a multiclass approach, where the target variable splits the patients in normal or total absence of any abnormal outcome (normal), patients with just an abnormal Bayley (ABN-Bayley) and patients with ASD diagnosis (ASD). It is important to notice that ASD is always associated with at least an abnormal Bayley language score (see Table 1). Therefore, this strategy has a target variable with three classes in order to assess if EEG dysmaturity features can discriminate abnormalities linked with ASD and Bayley abnormalities. Similarly to the two previous strategies, a classifier was designed via an LDA algorithm and with 3-fold testing (2/3 of data as training set and 1/3 test set). The hyperparameters were tuned using 10-fold cross-validation (9/10 of the training set is used for training set and 1/10 is used as validation set). The multiclass classifier was trained according to a one-versus-all scheme. Results were reported as classification error, Cohen's kappa score and two AUCs. The AUC_1 was computed as area under the ROC curve for the classification Abnormal Bayley Score vs All and AUC_2 was computed as area under the ROC curve for the ASD vs All. Similarly to the second strategy, different thresholds were tested for the Bayley score. The chosen range was [73,75,80], which represent the best and the worst case scenarios of the second strategy. An overview of the different classification performance metrics is reported in table 4. The statistical differences among features represented by three classes (Normal vs ABN-Bailey vs ASD) were tested with a Kruskal-Wallis test for each separate channel with an associated multiple comparison test.

2.5.4 Regression analysis for the Bayley score

The final strategy used a robust linear regression model to explain the three main Bayley scores. This aimed to investigate how the EEG dysmaturity features explain abnormalities of each score. For each of

the three Bayley scales, the five most correlated features were used to develop the robust model to predict the clinical score, together with the presence of TSC1 mutation. The regression results are reported in terms of explained variance (R2), mean absolute error (MAE) and the selected features for the regression.

Table 4. An overview of different classification and regression strategies used to detect development disorders abnormalities. In the case of simple binary classification, the positive class is represented by the ASD diagnosis (ASD vs NO ASD) and the performance metrics are the area under the curve, the Cohen's kappa and the misclassification error. In the second binary strategy, the positive class is represented by at least one development abnormality (ASD or abnormal Bayley Score) which is represented by one of the Bayley Scores under a certain threshold (ABN vs Normal). In case of multiclass classification, the first positive class is represented by patients with only an abnormal Bayley score, while the second positive class is the ASD patients (Normal vs ABN-Bayley vs ASD). Therefore, one obtains two AUCs: AUC1 for all vs patients with only an abnormal Bayley score and AUC2 for all vs patients with ASD. The last strategy is the regression between the EEG features and the BSID-III at two years. The common metrics are the coefficient of determination or explained variance (R2) and the mean absolute error (MAE).

Assessment strategies	**Target variable**	**Performance metrics**
Binary classification for ASD	ASD vs NO ASD	Error, AUC, Kappa Score
Binary Classification for abnormal development	Normal vs abnormal development	AUC, Kappa Score
Multiclass classification	Normal vs abnormal Bayley outcome (ABN – Bayley) vs ASD (ASD)	AUC_1 (ALL vs only abnormal Bayley outcome), AUC_2 (ALL vs ASD), Kappa Score
Regression	BSID-III variable	R2, MAE

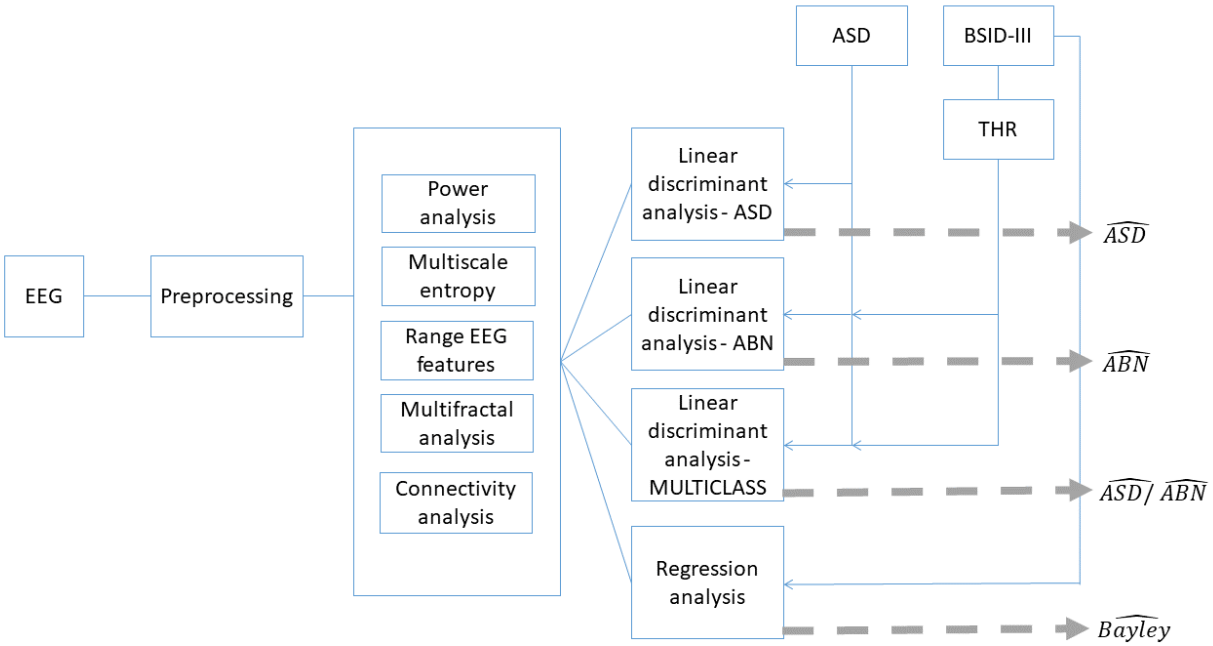


Figure 1. A schematic overview of the four strategies implemented in this study. The BSID-III stands for the Bayley Developmental Scale, ASD is autism spectrum disorder and THR is the threshold applied to define an abnormal Bayley outcome. After EEG preprocessing, a set of power, entropy, fractality, range EEG and connectivity features are derived to quantify the level of EEG dysmaturity. Those features are fed in different supervised discrimination strategies: 1) binary classification for ASD diagnosis with linear discriminant analysis (LDA), 2) binary classification with LDA for development abnormality diagnosis (ABN), 3) multiclass classification with LDA to determine if infants have ASD or if infants have only an abnormal BSID-III, 4) Regression analysis to extrapolate the Bayley score. The four supervised strategy blocks are fed with both features and the ground truth labels ASD, BSID-III (blue thin lines, BSID-III after threshold THR or the actual continuous variable for the regression analysis) and they have the prediction of ASD or abnormal outcome (dashed grey lines).

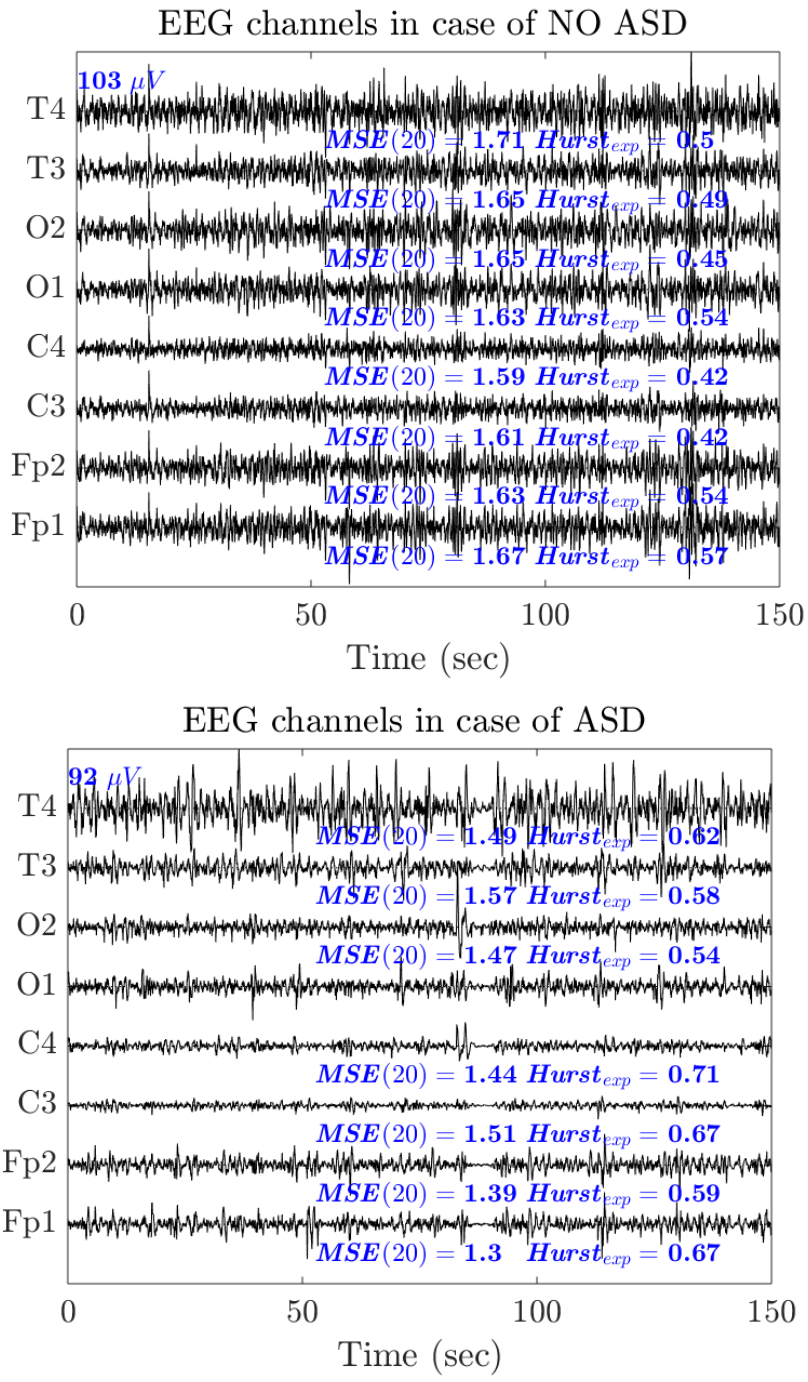


Figure 2. The figure shows two examples of EEG channels from the no ASD group (NO ASD, upper panel) and the autism spectrum disorder (ASD) group (lower panel). The data from the 8 channels are reported in a window of 150 sec and the associated entropy at scale 20 MSE(20) and the Hurst exponent are displayed if and only if the threshold criteria discussed in the text are met. The ASD EEG has lower entropy and higher Hurst exponent, which leads to a more discontinuous channel with slower rhythms. On the contrary, the EEG of a patient without ASD has faster frequencies and higher entropy at larger scale. Therefore, the ASD EEG can be considered a dysmature EEG. The sensitivity of the plotting is reported on the top left of the chart.

3. Results

The results of the quantitative EEG analysis were reported according to the different strategies explained in the section Methods.

3.1 Automatic Classification of ASD patients

Power, multifractal, entropy and connectivity features were computed to investigate if ASD was associated with a dysmature EEG and a linear discriminant analysis was used to automatically classify ASD patients. Figure 2 visually suggests that dysmature EEG predicted ASD symptoms at two years. This visual relationship is supported by the classification results described in the first strategy. Table 5 shows that the different LDA classifiers for the different feature subgroups have the AUCs in the range of 0.66 – 0.79 and the Cohen's kappa in the range of 0.26 - 0.48. The most important biomarkers in terms of AUC and kappa were MFA features (AUC(MFA) = 0.74, Kappa(MFA) = 0.48) and MSE features (AUC(MSE) = 0.79, Kappa(MSE) = 0.26).

Figure 3 shows the entropy at higher scale (MSE(20)) and regularity (Hurst-Exp) for the different channels. The Kruskal-Wallis test shows a significant lower entropy at higher scales for the following channels (F_{p1}– $p < 0.01, F_{p2}$– $p = 0.01, C_4$– $p = 0.04, T_3$– $p = 0.02$, T_4– $p < 0.01$) and higher regularity for the following channels (O_1– $p = 0.01, O_2$– $p = 0.05, T_4$– $p = 0.04$) in patients with an ASD diagnosis by 2 years of age.

Table 7 shows that the fractal and entropy features are specifically selected in the ASD classification when the entire pool of features is considered. In fact, all the attributes are either Hurst exponents or MSE features, like the complexity index and the entropy at scale 20.

Table 5 – Results for the binary classification models for ASD diagnosis (ASD vs NO ASD). The model was trained with *linear discriminant analysis* reported in terms of misclassification error (percentage of misdiagnosis, E(%)), area under the receiver operating characteristic (ROC) curve (AUC) and the agreement between machine and clinical labels via Cohen's Kappa. The different feature sets are predictive of the ASD diagnosis with areas under the ROC curve (AUC) close or higher than 70%. Cohen's Kappa is around 30% (or higher).

	Error (%)	**AUC**	**Kappa**
Power	32.59	0.66	0.27
MSE	33.01	0.79	0.26
rEEG	30.26	0.69	0.27
Conn	37.50	0.61	0.16
MFA	22.12	0.74	0.48
All	26.67	0.74	0.35

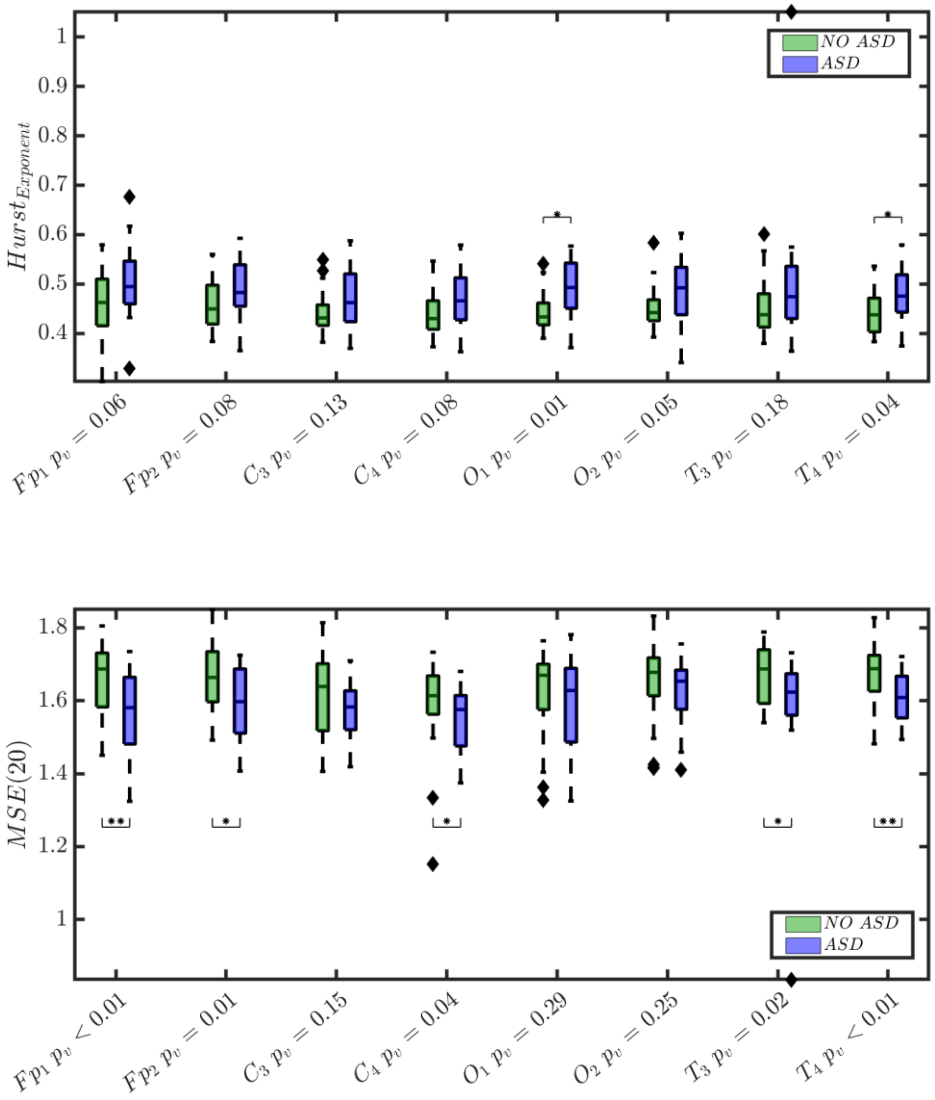


Figure 3. The figure shows the entropy at scale 20 MSE(20) and the Hurst exponent in the two groups (NO ASD = No ASD, ASD = Autism Spectrum Disorder). Both describe the persistence of slow-waves and discontinuity. In the case of ASD, the EEG presents a dysmature or disorganized pattern, since the regularity of the signal is higher due to spikiness, lack of smoothness and general discontinuity. The enhanced and abnormal slow-wave information in the disorganized EEG lowers the entropy at lower frequencies (MSE(20)). P-values have been derived with Kruskal-Wallis test. The symbols * and ** respectively represent post-hoc comparison with p-value <= 0.05 and <=0.01.

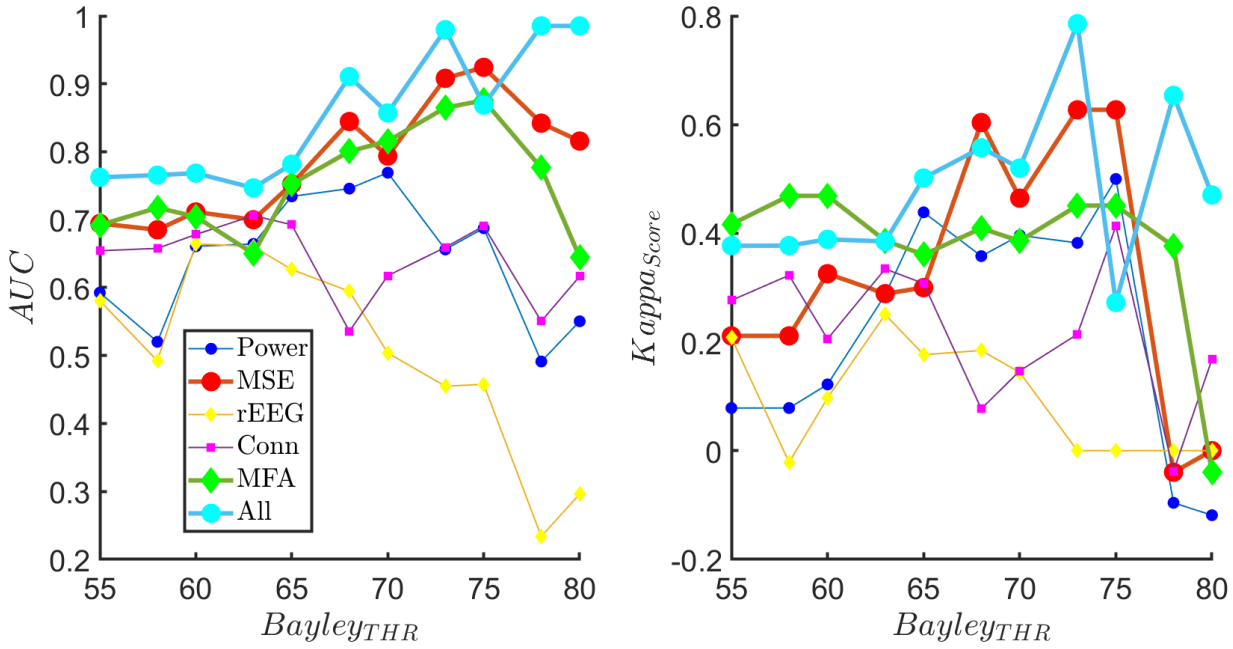


Figure 4. Binary classification performance in function of the threshold applied to BSID-III (BayleyTHR) to define the positive class. The two panels report the *linear discriminant analysis* area under the ROC curve (AUC) and Kappa score for the classification of the normal vs abnormal development group for each group of features. The abnormal group contains at least one developmental problem (ASD or abnormal Bayley). The Bayley Threshold has been used to define the abnormal Bayley outcome for each of the three investigated scores (cognitive, motor and language outcome). The reported groups of features are power, entropy (MSE), range-EEG or NEURAL features (rEEG), connectivity (Conn), fractality (MFA) and all the features combined (All). Each AUC and Kappa score chart is reported in different colors and different symbols for each feature group.

3.2 Automatic Classification of abnormal outcomes

The same features were used in another LDA model to automatically classify abnormal development outcome according to different Bayley score thresholds. Figure 4 reports the results of the LDA classification of the abnormal outcomes based on dysmature EEG. The AUCs and kappa scores are reported for the tested range of Bayley thresholds to define abnormalities in the development. The second strategy confirms that MSE (red-circles curve) and MFA (green-diamonds curve) outperform the other biomarkers in the prediction of abnormal development outcome. For most of the thresholds, MSE and MFA report the highest AUC and Kappa. The peak-performances are reached at a threshold of 75: MSE reaches AUC up to 0.92 and Kappa up to 0.63, while MFA reaches AUC up to 0.88 and Kappa score up to 0.45. Beyond this 75 threshold, a drop in classification performance of each feature group has been observed except for the combination of all features.

3.3 Multiclass analysis of abnormal Bayley outcomes, ASD and normal patients

Eventually, the same pool of features was used to automatically discriminate normal patients, ASD patients and patients with only abnormal Bayley outcome. The results associated to the multiclass

strategy are reported in Table 6. The findings of the third strategy are reported for the Bayley thresholds 73,75,80, which represent the peak and the drop of performance in the second strategy (Figure 4). In case of the multiclass approach, there is a steady increase of all parameters (AUC_1, AUC_2, Kappa) with increasing threshold, but the values of AUC_2consistently score higher than those of AUC_1. For example, AUC_2 for MSE, MFA and all features together are 0.75, 0.71, 0.74 respectively, while AUC_1 are 0.65, 0.71, 0.73 respectively. This means that the ASD diagnosis score seems easier to discriminate compared to a simple abnormality in BSID-III.

Figure 5 depicts the boxplots for MSE(20) and Hurst-Exp in the three different groups defined for the multiclass problem (Normal vs ABN Bailey vs ASD). The Kruskal-Wallis test shows a significant difference for lower entropy at higher scales in the following channels ($F_{p1}- \ p \ < \ 0.01, F_{p2}- \ p \ = \ 0.01, T_3- \ p \ = \ 0.02, T_4- \ p \ = \ 0.02$) and higher regularity for the following channels ($O_1 \ - \ p \ = \ 0.03, O_2- \ p \ = \ 0.05$). The multicomparison test shows a tendency associated to the severity of abnormal development at 2 years for the MSE(20) in Fp1, as indicated by the asterisks associated to p <= 0.05. The remaining channels with a significant p-value show a significant difference between normal patients and ASD. The entropy at scale 20 is lower in case of an ASD patient with abnormal Bayley, while the Hurst regularity increases in case of ASD.

Table 7 shows the selected features for the binary classification when the entire pool of features is considered. They mostly belong to the fractal and entropy family with the addition of graph and network resilience features in the δ_2 band. Figure 7 shows the boxplots of the number of superfluous connections (or network resilience), which suggest a higher network resilience is found in case of abnormal developmental outcome, as confirmed by the Kruskal-Wallis test for δ_2 (p = 0.02), θ (p = 0.04) and α (p=0.03). The boxplots were reported by assuming an abnormal development with Bayley score below 80.

Table 6 – Results for the multiclass classification to discriminate patient with normal development, ASD and patients with only abnormal development (Normal vs ASD vs ABN Bayley). The model was trained with *linear discriminant analysis*. The performance is reported in terms of misclassification error (percentage of misdiagnosis, E (%)), area under the receiver operating characteristic (ROC) curve (AUC) and the agreement between machine and clinical labels via Cohen's Kappa. Since the model was trained according to the OneVsAll scheme, the two reported AUCs represent the AUCs of the class with only development abnormalities vs all (AUC_1) and AUC of the combination of ASD vs all (AUC_2). The results are reported for entropy (MSE), fractality (MFA) and the combination of all features. The performance is reported for the Bayley score threshold range [73,75,80] to define the development delay.

Bayley	**Error (%)**	**AUC1**	**AUC2**	**Kappa**
	MSE			
73	36.67	0.60	0.72	0.28
75	43.33	0.55	0.67	0.13
80	30.00	0.65	0.75	0.36
	MFA			
73	33.33	0.66	0.66	0.36
75	33.33	0.65	0.73	0.36
80	30.00	0.71	0.71	0.41
	All			
73	35.90	0.69	0.76	0.33
75	35.90	0.71	0.76	0.32
80	33.33	0.73	0.74	0.35

Table 7 – Selected features for the binary classification of NO ASD vs ASD and the multiclass scenario when all features are combined together. The results for the multiclass design are reported for the Bayley score threshold range [73,75,80] to define the development delay. CI stands for Complexity Index, while Nsup is the number of superfluous connections of the Scalp-EEG network as explained in the main text.

Bayley	Features				
	Binary				
	Hurst(O1)	CI(T4)	CI(O1)	MSE(20,T4)	MSE(20,Fp1)
	Multiclass				
73	Hurst(O1)	CI(T4)	CI(O1)	Nsup (δ_2)	PathLength(δ_2)
75	Hurst(O1)	CI(T4)	CI(O1)	Nsup (δ_2)	PathLength(δ_2)
80	Hurst(O1)	Nsup(δ_2)	CI(T4)	CI(O1)	PathLength(δ_2)

3.4 Regression analysis for the Bayley score

The last step of this study was the regression analysis to automatically compute the different Bayley scores with quantitative EEG features. The relationship between the different Bayley outcome and the EEG dysmature features is reported in Table 8. The explained variance or coefficient R^2 for the Motor, Language and Cognitive score is respectively 0.30, 0.38, 0.46, while the mean absolute error is 7.85, 7.5 and 7.85. For each of the models, the five most correlated features with different Bayley scores which were used in the final model are also reported in Table 8, alongside the TSC mutation variable. Similarly to the classification strategies, the entropy at scale 20 (MSE(20,Fp1)) and the Hurst exponent contribute to define the Bayley score at 2 years. Figure 6 shows the relationship between MSE(20)/HurstExp and the cognitive Bayley score.

Table 8 – Regression model to predict the BSID-III score with the most correlated features and the presence of TSC mutation. The features reported here represent the best model to explain the score in terms of mean absolute error and coefficient determination (R^2). The first column reports the type of Bayley score, the second column the involved features, while the last ones report the regression performance (R^2, MAE and the associated p-value).

Bayley	**Features**	R^2	**MAE**	**Pval**
Motor	MSE(20,T4),Ratio(δ_1),MSE(20,O1), MSE(20,Fp1),PathLength(δ_1), TSC	0.3048	7.8502	0.0068
LANG	ΔH (C3),C3(T3),C3(C3),HurstExp(C4), HurstExp((O1), TSC	0.3711	7.5014	0.0008
COG	Diff(δ),SD(δ),MSE(20,Fp2), Width(Beta), Width(δ), TSC	0.4564	7.8529	0.0002

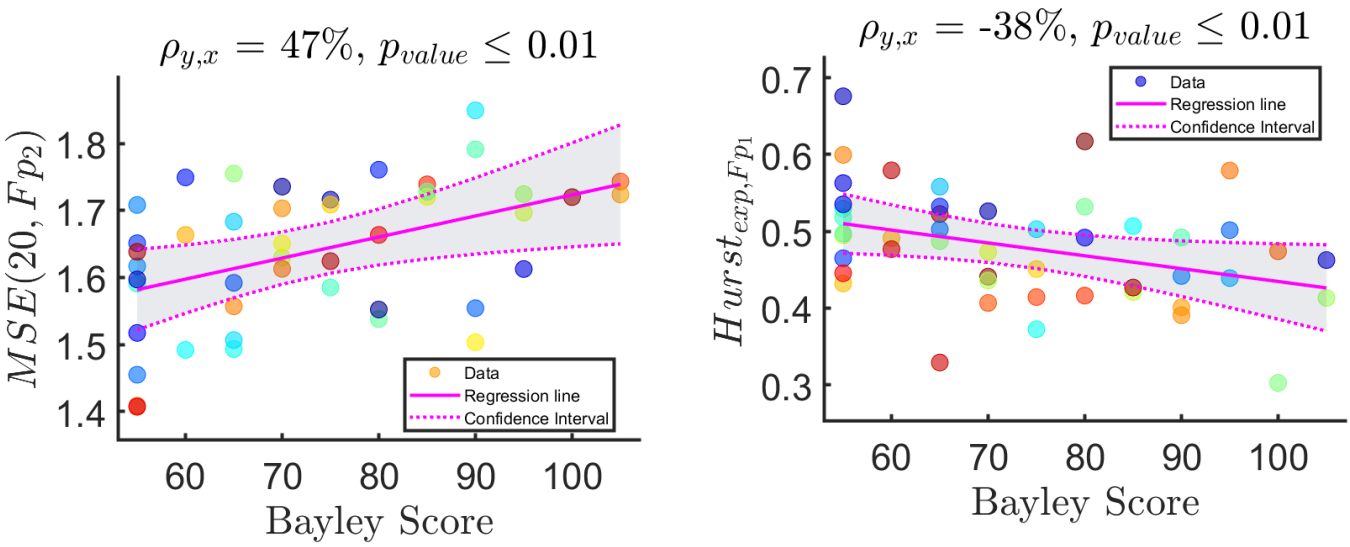


Figure 6. The figure shows the entropy at scale 20 MSE(20) and the Hurst exponent in function of the Cognitive BSID-III score. The two panels reported the cluster of data points (circles with a color for each patient), the expected value of the considered feature for each Bayley score (pink thick line) and the 95% confidence intervals (pink dashed lines). The left panel clearly shows that the higher the Bayley score the higher the entropy at scale 20, while the right panel shows that the higher the cognitive score the lower the Hurst exponent. The figure confirms that both entropy and the regularity are features of brain dysmaturity, and are related to developmental outcome in ASD subjects. In addition, the increase of MSE(20) underlines how the persistence of slow-waves is related to a worse developmental outcome.

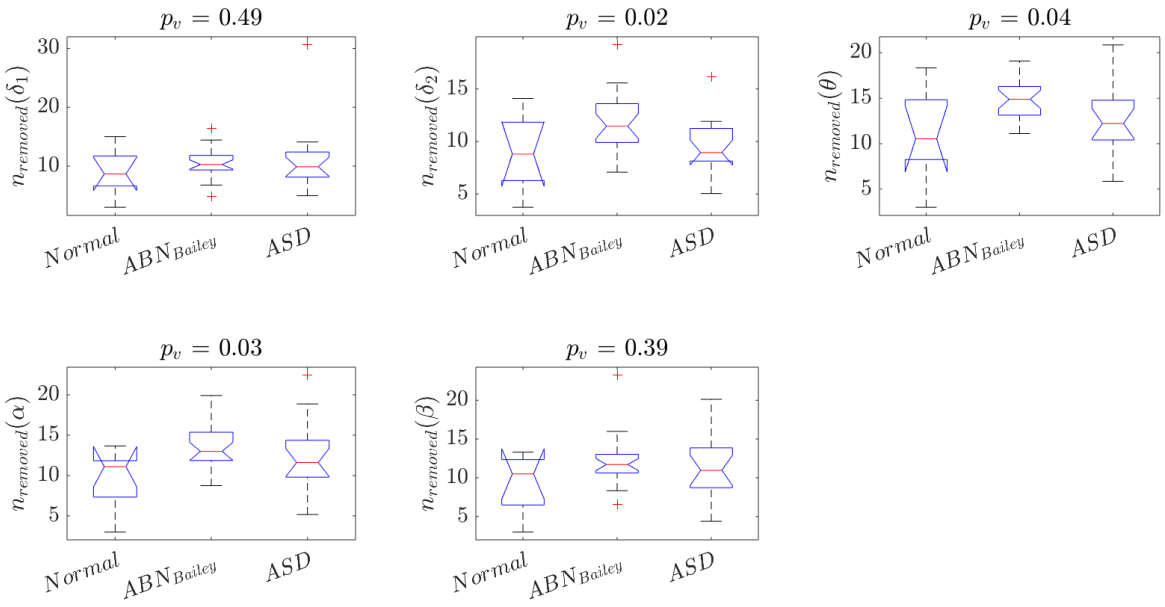


Figure 7. The measure of network redundancy is shown for the three different study groups: normal, abnormal Bayley outcome (Bayley < 80) and ASD with an abnormal Bayley. As shown by the second and third panel, the number of superfluous connections (nsup or Nremoved) is higher in case of development abnormalities.

4 Discussion

The quantitative analysis of EEG background confirmed that an early-life abnormal or dysmature EEG background is associated with an abnormal development outcome in TSC infants. The current findings do not only support that quantitative EEG analysis in the first months of life can be helpful for automatic ASD diagnosis, but they also confirm the similarities between EEG dysmaturity and the ASD patients' EEG, which are normally investigated only in the later childhood.

The results of the models of the first and second strategy show that a dysmature EEG in the first months of life is associated with ASD traits at 24 months and with neurodevelopmental abnormalities. Table 5 underlines that dysmature EEG features can discriminate ASD patients, as also displayed in figure 2. Those results are comparable to the ASD siblings reported by (Bosl et al., 2011) at 6 months. Although the current results might underperform compared to more common studies related to classification of ASD (Billeci et al., 2013; Duffy & Als, 2012; Peters et al., 2013), the literature has normally focused on children older than 2 years, while this study has specifically focused to young infants below 4 months. Furthermore, Figure 4 and Table 6 do not only stress that these same features can detect abnormal development as shown by a wide range of studies in neonates (Okumura et al., 2002; Watanabe et al., 1999), but they can discriminate can discriminate ASD patients from patients with abnormal Bayley scores. As further proof of the relationship between abnormal Bayley and EEG dysmaturity, we showed that characteristic quantitative EEG features were significantly able to explain the variance of the cognitive, language and motor BSID-III score (Table 8 and Figure 6). Interestingly, the reported analysis also inferred the best cut-off for the Bayley to define problems with the development based on data-driven methods. The best BSID-III threshold to discriminate healthy patients from controls seems to be

75 for the binary case and 80 for the multiclass case, in line with other clinical studies (Duncan et al., 2015; Johnson et al., 2014).

Our findings suggest that the most informative features to discriminate ASD in TSC is MSE and MFA, as shown by (Ahmadlou, Adeli, & Adeli, 2012; Bosl et al., 2011) and by the performance in Table 5 and 6, the selected features in Table 7 and the red and green charts in Figure 4. Those results do not only confirm known results of the risk of autism (Billeci et al., 2013), but prove that ASD-prone patients and subjects with an abnormal Bayley score have a dysmature early-life EEG, as defined by (Pavlidis, Lloyd, Mathieson, & Boylan, 2017) and quantified by (De Wel et al., 2017; González et al., 2011; M. Lavanga, De Wel, Caicedo, Heremans, et al., 2017; M Lavanga et al., 2018; J. M. O'Toole, Boylan, Vanhatalo, & Stevenson, 2016). This type of signal is characterized by a lower complexity and higher discontinuity at very young age (< 4 months) (see Figure 3) and it is associated with adverse outcome (Pavlidis, Lloyd, & Boylan, 2017). Figure 5 might also suggest that EEG entropy at higher scale decreases even further in case of ASD compared to just a lower developmental outcome (especially in channel Fp1). In addition, the selected features for both the classification and the regression models (Table 7 and 8) emphasize the role of lower frequencies for predicting developmental delay, which further support the persistence of EEG slow-waves in case of dysmaturity or poor developmental outcome. The fact that the lower complexity and higher regularity play a role in the detection of the poor outcome is confirmed by the regression results: a lower entropy and higher regularity in neonatal EEG lead to a worse developmental outcome in later life (Table 8). Interestingly, a higher EEG network resilience was also found in case of developmental abnormality (Figure 7), which confirms the results reported by Peters (Peters et al., 2013).

Based on the current results, the quantitative EEG analysis can provide insights on the neurobiology of the altered brain maturation in patients with TSC. The higher network resilience found in case of development abnormalities, as reported by Figure 7 and Peters et al., might be a consequence of local over-connectivity or reduced functional specialization in ASD patients (Peters et al., 2013). The dysmature neonatal EEG background is associated with a poor cognitive outcome (Biagioni et al., 1996; Le Bihannic et al., 2012; Okumura et al., 2002; Daniele Selton et al., 2010) and Table 8 and Figure 6 confirms that a lower Bayley score is associated with an early-life abnormal EEG in young TSC infants. Specifically, a background EEG with a lower entropy, higher regularity and higher width of the range EEG is predictive of lower cognitive, motor and language outcomes. More importantly, TSC patients with abnormal development can be discriminated based on automatic biomarkers of the early-life EEG. The current results further claim that a dysmature EEG pattern might reflect cortical injury or a maturation delay in the development of neurons (Hayakawa et al., 1997; Le Bihannic et al., 2012; Selton et al., 2010) or simply, the EEG of TSC patients with ASD is associated to a dysmature EEG, as it is the case for premature infants with a poor developmental outcome. Unlike other studies related to ASD (Bosl et al., 2011; Peters et al., 2013), the current research includes infants with age below 4 months and an automatic analysis of early-life EEG might be a pivotal tool to prevent and preserve the future development of the infant, as also shown in a recent review (Kong et al., 2018).

However, it is also important to point out the limitations of the current study. The number of ASD patients is limited and future validation studies should include a bigger sample to confirm the current results. Furthermore, the quantitative analysis pursued a different nested strategy to show that a dysmature EEG background is specifically predictive of ASD diagnosis and developmental abnormalities and the obtained kappa score shows a moderate association between features and outcomes. However,

the moderate level might be also caused by the poor communication skills of ASD patients, which entails a lower Bayley language score (as seen by the values well below 70 in Table 1) . Therefore, the ASD class might be difficult to discriminate from a generic abnormal Bayley score. A more interesting problem could be the prediction of intellectual disability in ASD patients (normally defined by cognitive scores< 70) compared to ASD patients with any cognitive problem. However, a bigger sample size of ASD patients would be required for this type of analysis. Moreover, an abnormal Bayley outcome might include patients with just a lower developmental motor outcome (known also as developmental dissociation) or patients with both intellectual disability and developmental dissociation. Future studies should also include a proper investigation of how the different aspects and traits of the dysmature EEG contribute in the definition of different abnormal Bayley outcomes.

In a nutshell, the current analysis delved into the association of a dysmature EEG background in TSC neonates and infants, the later diagnosis of ASD and its interplay with the developmental outcome at 2 years. Both entropy and fractal features can indeed discriminate ASD at early-age, but it can be simply the consequence of a worsening developmental outcome. And yet, MSE and MFA have been proven able to discriminate ASD from general development abnormalities in a multiclass scenario. Besides, multiple studies have shown that dysmature EEG predicts a worse developmental outcome, but the current studies show which of the early-EEG quantitative features correlate with the Bayley score at 2 years.

Conclusion

The investigation of the quantitative EEG analysis in TSC infants showed that discontinuity and dysmaturity of early-life EEG is associated with ASD diagnosis and neurodevelopmental abnormalities at the age of 2 years. Following the definition of Pavlidis and other pioneering studies on the autism spectrum disorder EEG, a dysmature EEG is characterized by low entropy and high regularity as a consequence of the discontinuity and the persistence of slow-waves. Those features are also the ones that are most predictive in detecting ASD or other abnormal neurodevelopmental outcomes, such as a lower cognitive, language or motor DQ's. In addition, a larger network resilience has also been found in case of development abnormalities (Peters et al., 2013). Similarly, to other clinical studies, the definition of abnormal development was based on a Bayley Score threshold. Surprisingly, the value that led to the best binary and multiclass classification was in a range between [75-80], which are near the most common thresholds used in the clinical practice. Eventually, the quantitative EEG analysis at early-stage might provide a greater understanding of the brain functional processing for cognitive disorders or development disabilities such as autism spectrum disorder. The quantitative EEG analysis at the cot-side might lead to a further tuning of interventions or preventive care in case of deviation from the normal developmental trajectory.

Conflict of interest statement

The authors declare that the research was conducted in the absence of any commercial or financial relationships that could be construed as a potential conflict of interest.

Acknowledgements

Research supported by Bijzonder Onderzoeksfonds KU Leuven (BOF) : C24/15/036 ``The effect of perinatal stress on the later outcome in preterm babies", imec sbo funds "Wearablehealth", EU: H2020 MSCA-ITN-2018: 'INtegrating Functional Assessment measures for Neonatal Safeguard (INFANS)',

funded by the European Commission under Grant Agreement #813483. This research received funding from the Flemish Government under the “Onderzoeksprogramma Artificiële Intelligentie (AI) Vlaanderen” programme. Mario Lavanga is a SB Ph.D. fellow at Fonds voor Wetenschappelijk Onderzoek (FWO), Vlaanderen, supported by the Flemish government. The EPISTOP study was funded by the 7th Framework Programme of European Commission within the Large-scale Integrating Project EPISTOP (Grant Agreement number 602391). The authors would like to thank you the remaining members of the EPISTOP Consortium: J. Anink, A. Benvenuto, M. Blazejczyk, A. Bongaarts, J. Borkowska D. Breuillard, D. Chmielewski, M. Dabrowska, L. Emberti Gialloreti, K. Giannikou, J. Głowacka-Walas, L. Hamieh, A. Haręza, H. Hulshof, A. Iyer, B. Janssen, J. Jaworski, K. Lehmann, K. Lemmens A. Leusman, N. Maćkowiak, J.D. Mills, A. Muehlebner, K. Sadowski, C. Scheldeman, T. Scholl, M. Schooneveld, A. Sciuto, K. Sijko, M. Slowinska, A. Tempes, M. Urbańska, J. van Scheppingen, B. Verhelle, J. Vervisch.

Appendix A

A.1 EEG Network resilience

The resilience has been derived as the number of superfluous connections n_{sup}, which are the connections that can be removed without significant in the EEG network. Suppose we order all the connections in descending order based on the intensity of the coupling. Suppose also the set of original weights is defined as ${w_{ij}}^0$. The number n_{sup} of superfluous connections is derived as the number that maximizes the following quantity

$$n_{sup} = \max_n H\left(w_{ij}(n)\right) + E\left(w_{ij}(n)\right) = -\sum_{ij} w_{ij}(n) \log w_{ij}(n) + \sum_{ij} (w_{ij}(n) - {w_{ij}}^0)^2$$

where $H\left(w_{ij}(n)\right)$ is the entropy of the network where n weights were removed. The values $w_{ij}(n)$ represent the remaining non-zero weights, while $E\left(w_{ij}(n)\right)$ is the squared error between the new set of weights and the original one (Mario Lavanga, Bollen, et al., 2020) (Mario Lavanga, Smets, et al., 2020). The number n_{sup} represents the highest number of removed connections that maintain the global connectivity high without significant deviation from the original matrix. The optimization is to remove as many connections as possible, which results in an increasing error and decreasing connectivity entropy. In an extreme scenario, a redundant network keeps the global entropy high even if there are a few non-zero couplings in the matrix; and, in general, they will have a higher n_{sup}.

References

Ahmadlou, M., Adeli, H., & Adeli, A. (2012). Improved visibility graph fractality with application for the diagnosis of Autism Spectrum Disorder. *Physica A*, *391*(20), 4720–4726. https://doi.org/10.1016/j.physa.2012.04.025

Biagioni, E., Bartalena, L., Biver, P., Pieri, R., & Cioni, G. (1996). Electroencephalographic Dysmaturity in Preterm Infants: A Prognostic Tool in the Early Postnatal Period. *Neuropediatrics*, *27*(06), 311–316. https://doi.org/10.1055/s-2007-973800

Billeci, L., Sicca, F., Maharatna, K., Apicella, F., Narzisi, A., Campatelli, G., … Muratori, F. (2013, July 18).

On the application of Quantitative EEG for characterizing autistic brain: A systematic review. *Frontiers in Human Neuroscience*, Vol. 7, p. 442. https://doi.org/10.3389/fnhum.2013.00442

Bortel, R., & Sovka, P. (2007). Approximation of statistical distribution of magnitude squared coherence estimated with segment overlapping. *Signal Processing*, *87*, 1100–1117. https://doi.org/10.1016/j.sigpro.2006.10.003

Bosl, W., Tierney, A., Tager-Flusberg, H., & Nelson, C. (2011). EEG complexity as a biomarker for autism spectrum disorder risk. *BMC Medicine*, *9*(1), 18. https://doi.org/10.1186/1741-7015-9-18

Bullmore, E., & Sporns, O. (2009). Complex brain networks: graph theoretical analysis of structural and functional systems. *Nature Reviews Neuroscience*, *10*(3), 186–198. https://doi.org/10.1038/nrn2575

Chen, Y. W., & Lin, C. J. (2006). Combining SVMs with various feature selection strategies. *Studies in Fuzziness and Soft Computing*, *207*, 315–324. https://doi.org/10.1007/978-3-540-35488-8_13

Costa, M., Goldberger, A. L., & Peng, C. K. (2002). Multiscale entropy analysis of complex physiologic time series. *Phys Rev Lett*, *89*(6), 68102. Retrieved from http://www.ncbi.nlm.nih.gov/entrez/query.fcgi?cmd=Retrieve&db=PubMed&dopt=Citation&list_uids=12190613

Curatolo, P. (2015, March 1). Mechanistic target of rapamycin (mTOR) in tuberous sclerosis complex-associated epilepsy. *Pediatric Neurology*, Vol. 52, pp. 281–289. https://doi.org/10.1016/j.pediatrneurol.2014.10.028

De Wel, O., Lavanga, M., Dorado, A., Jansen, K., Dereymaeker, A., Naulaers, G., & Van Huffel, S. (2017). Complexity Analysis of Neonatal EEG Using Multiscale Entropy: Applications in Brain Maturation and Sleep Stage Classification. *Entropy*, *19*(10), 516. https://doi.org/10.3390/e19100516

Duffy, F. H., & Als, H. (2012). A stable pattern of EEG spectral coherence distinguishes children with autism from neuro-typical controls - a large case control study. *BMC Medicine*, *10*(1), 64. https://doi.org/10.1186/1741-7015-10-64

Duncan, A. F., Bann, C., Boatman, C., Hintz, S. R., Vaucher, Y. E., Vohr, B. R., … Heyne, R. J. (2015). Do currently recommended Bayley-III cutoffs overestimate motor impairment in infants born <27 weeks gestation? *Journal of Perinatology*, *35*(7), 516–521. https://doi.org/10.1038/jp.2014.243

Floyd, S., & Warmuth, M. (1995). Sample compression, learnability, and the Vapnik-Chervonenkis dimension. *Machine Learning*, *21*(3), 269–304. https://doi.org/10.1007/BF00993593

González, J. J., Mañas, S., De Vera, L., Méndez, L. D., López, S., Garrido, J. M., & Pereda, E. (2011). Assessment of electroencephalographic functional connectivity in term and preterm neonates. *Clinical Neurophysiology*, *122*(4), 696–702. https://doi.org/10.1016/j.clinph.2010.08.025

Hayakawa, F., Okumura, A., Kato, T., Kuno, K., & Watanabe, K. (1997). Dysmature EEG pattern in EEGs of preterm infants with cognitive impairment: Maturation arrest caused by prolonged mild CNS depression. *Brain and Development*, *19*(2), 122–125. https://doi.org/10.1016/S0387-7604(96)00491-3

Hellström-Westas, L. (2006, September). Continuous Electroencephalography Monitoring of the Preterm Infant. *Clinics in Perinatology*, Vol. 33, pp. 633–647. https://doi.org/10.1016/j.clp.2006.06.003

Hoyer, D., Tetschke, F., Jaekel, S., Nowack, S., Witte, O. W., Schleußner, E., & Schneider, U. (2013). Fetal Functional Brain Age Assessed from Universal Developmental Indices Obtained from Neuro-Vegetative Activity Patterns. *PLoS ONE*, *8*(9), 1–8. https://doi.org/10.1371/journal.pone.0074431

Isler, J. R., Stark, R. I., Grieve, P. G., Welch, M. G., & Myers, M. M. (2018). Integrated information in the EEG of preterm infants increases with family nurture intervention, age, and conscious state. *PLOS ONE*, *13*(10), e0206237. https://doi.org/10.1371/journal.pone.0206237

Jaffard, S., Lashermes, B., & Abry, P. (2006). Wavelet leaders in multifractal analysis. *Wavelet Analysis and Applications*, 201–246. https://doi.org/10.1007/978-3-7643-7778-6_17

Johnson, S., Moore, T., & Marlow, N. (2014). Using the Bayley-III to assess neurodevelopmental delay: Which cut-off should be used? *Pediatric Research*, *75*(5), 670–674. https://doi.org/10.1038/pr.2014.10

Kaffashi, F., Scher, M. S., Ludington-Hoe, S. M., & Loparo, K. A. (2013). An analysis of the kangaroo care intervention using neonatal EEG complexity: A preliminary study. *Clinical Neurophysiology*, *124*(2), 238–246. https://doi.org/10.1016/j.clinph.2012.06.021

Kesić, S., & Spasić, S. Z. (2016). Application of Higuchi's fractal dimension from basic to clinical neurophysiology: A review. *Computer Methods and Programs in Biomedicine*, *133*, 55–70. https://doi.org/10.1016/j.cmpb.2016.05.014

Kong, A. H. T., Lai, M. M., Finnigan, S., Ware, R. S., Boyd, R. N., & Colditz, P. B. (2018). Background EEG features and prediction of cognitive outcomes in very preterm infants: A systematic review. *Early Human Development*, *127*, 74–84. https://doi.org/10.1016/J.EARLHUMDEV.2018.09.015

Lake, D. E., & Moorman, J. R. (2011). Accurate estimation of entropy in very short physiological time series: the problem of atrial fibrillation detection in implanted ventricular devices. *American Journal of Physiology. Heart and Circulatory Physiology*, *300*(1), H319–H325. https://doi.org/10.1152/ajpheart.00561.2010

Lavanga, M., De Wel, O., Caicedo, A., Heremans, E., Jansen, K., Dereymaeker, A., … Van Huffel, S. (2017). Automatic quiet sleep detection based on multifractality in preterm neonates: Effects of maturation. *Proceedings of the 39th Annual International Conference of the IEEE Engineering in Medicine and Biology Society (EMBC)*, 2010–2013. https://doi.org/10.1109/EMBC.2017.8037246

Lavanga, M., De Wel, O., Caicedo, A., Jansen, K., Dereymaeker, A., Naulaers, G., & Van Huffel, S. (2017). Monitoring Effective Connectivity in the Preterm Brain: A Graph Approach to Study Maturation. *Complexity*, *2017*. https://doi.org/10.1155/2017/9078541

Lavanga, M, De Wel, O., Caicedo, A., Heremans, E., Jansen, K., Dereymaeker, A., … Van Huffel, S. (2017). Automatic quiet sleep detection based on multifractality in preterm neonates: Effects of maturation. *2017 39th Annual International Conference of the IEEE Engineering in Medicine and Biology Society (EMBC)*, 2010–2013. https://doi.org/10.1109/EMBC.2017.8037246

Lavanga, M, Wel, O. De, Caicedo, A., Jansen, K., Dereymaeker, A., Naulaers, G., & Huffel, S. Van. (2018). A brain-age model for preterm infants based on functional connectivity. *Physiological Measurement*, *39*(4), 044006. https://doi.org/10.1088/1361-6579/AABAC4

Lavanga, Mario, Bollen, B., Jansen, K., Ortibus, E., Naulaers, G., Van Huffel, S., & Caicedo, A. (2020). A bradycardia-based stress calculator for the neonatal intensive care unit: a multisystem approach. *Frontiers in Physiology*, *11*, 741. https://doi.org/10.3389/FPHYS.2020.00741

Lavanga, Mario, De Wel, O., Caicedo, A., Jansen, K., Dereymaeker, A., Naulaers, G., & Van Huffel, S. (2018). A brain-age model for preterm infants based on functional connectivity. *Physiological Measurement*, *39*(4), 044006. https://doi.org/10.1088/1361-6579/aabac4

Lavanga, Mario, Smets, L., Bollen, B., Jansen, K., Ortibus, E., Van Huffel, S., … Caeicedo, A. (2020). A perinatal stress calculator for the neonatal intensive care unit: an unobtrusive approach. *Physiological Measurement*, 1–26.

Le Bihannic, A., Beauvais, K., Busnel, A., de Barace, C., & Furby, A. (2012). Prognostic value of EEG in very premature newborns. *Archives of Disease in Childhood. Fetal and Neonatal Edition*, *97*(2), F106-9. https://doi.org/10.1136/adc.2010.204735

Moavero, R., Benvenuto, A., Emberti Gialloreti, L., Siracusano, M., Kotulska, K., Weschke, B., … on behalf of the EPISTOP Consortium. (2019). Early Clinical Predictors of Autism Spectrum Disorder in Infants with Tuberous Sclerosis Complex: Results from the EPISTOP Study. *Journal of Clinical Medicine*, *8*(6), 788. https://doi.org/10.3390/jcm8060788

Nolte, G., Bai, O., Wheaton, L., Mari, Z., Vorbach, S., & Hallett, M. (2004). Identifying true brain interaction from EEG data using the imaginary part of coherency. *Clinical Neurophysiology*, *115*(10), 2292–2307. https://doi.org/10.1016/j.clinph.2004.04.029

O'Toole, J. M., & Boylan, G. B. (2017). NEURAL: quantitative features for newborn EEG using Matlab. *ArXiv Preprint ArXiv:1704.05694*. Retrieved from http://arxiv.org/abs/1704.05694

O'Toole, J. M., Boylan, G. B., Vanhatalo, S., & Stevenson, N. J. (2016). Estimating functional brain maturity in very and extremely preterm neonates using automated analysis of the electroencephalogram. *Clinical Neurophysiology*. https://doi.org/10.1016/j.clinph.2016.02.024

O'Toole, John M., Pavlidis, E., Korotchikova, I., Boylan, G. B., & Stevenson, N. J. (2019). Temporal evolution of quantitative EEG within 3 days of birth in early preterm infants. *Scientific Reports*, *9*(1). https://doi.org/10.1038/s41598-019-41227-9

Okumura, A., Hayakawa, F., Kato, T., Watanabe, K., & Kuno, K. (2002). Developmental outcome and types of chronic-stage EEG abnormalities in preterm infants. *Developmental Medicine and Child Neurology*, *44*(11), 729–734. https://doi.org/10.1017/S0012162201002845

Pavlidis, E., Lloyd, R. O., & Boylan, G. B. (2017). EEG-A Valuable Biomarker of Brain Injury in Preterm Infants. *Developmental Neuroscience*, *39*(1–4), 23–35. https://doi.org/10.1159/000456659

Pavlidis, E., Lloyd, R. O., Mathieson, S., & Boylan, G. B. (2017). A review of important electroencephalogram features for the assessment of brain maturation in premature infants. *Acta Paediatrica*, *106*(9), 1394–1408. https://doi.org/10.1111/apa.13956

Peters, J. M., Taquet, M., Vega, C., Jeste, S. S., Fernández, I. S., Tan, J., … Warfield, S. K. (2013). Brain functional networks in syndromic and non-syndromic autism: a graph theoretical study of EEG connectivity. *BMC Medicine*, *11*(1), 54. https://doi.org/10.1186/1741-7015-11-54

Popivanov, D., Stomonyakov, V., Minchev, Z., Jivkova, S., Dojnov, P., Jivkov, S., … Kosev, S. (2006). Multifractality of decomposed EEG during imaginary and real visual-motor tracking. *Biological Cybernetics*, *94*(2), 149–156. https://doi.org/10.1007/s00422-005-0037-5

Rubinov, M., & Sporns, O. (2010a). Complex network measures of brain connectivity: Uses and interpretations. *NeuroImage*, *52*(3), 1059–1069.

https://doi.org/10.1016/j.neuroimage.2009.10.003

Rubinov, M., & Sporns, O. (2010b). Complex network measures of brain connectivity: Uses and interpretations. *NeuroImage*, *52*(3), 1059–1069. https://doi.org/10.1016/j.neuroimage.2009.10.003

Selton, D., Andre, M., Debruille, C., Deforge, H., & Hascoët, J. M. (2013). Cognitive outcome at 5years in very premature children without severe early cerebral abnormalities: Relationships with EEG at 6 weeks after birth. *Neurophysiologie Clinique*, *43*(5–6), 289–297. https://doi.org/10.1016/j.neucli.2013.09.003

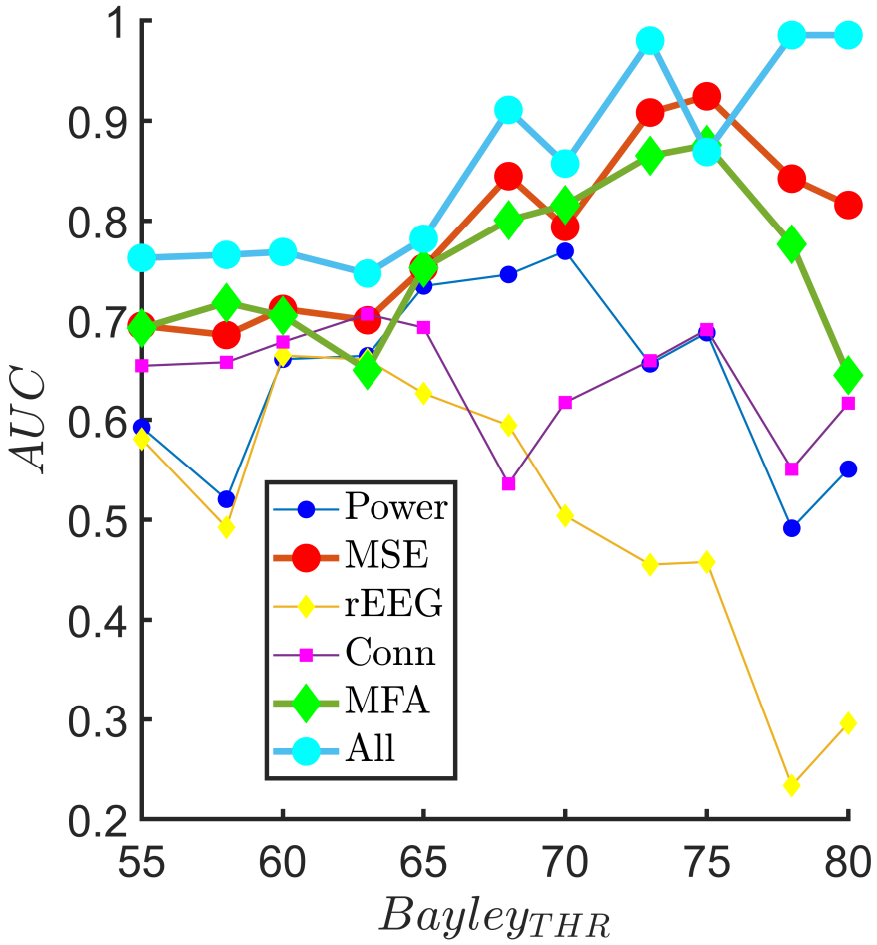
Selton, Daniele, André, M., Debruille, C., Deforge, H., Fresson, J., & Hascoet, J. M. (2010). EEG at 6 weeks of life in very premature neonates. *Clinical Neurophysiology*, *121*(6), 818–822. https://doi.org/10.1016/j.clinph.2009.11.006

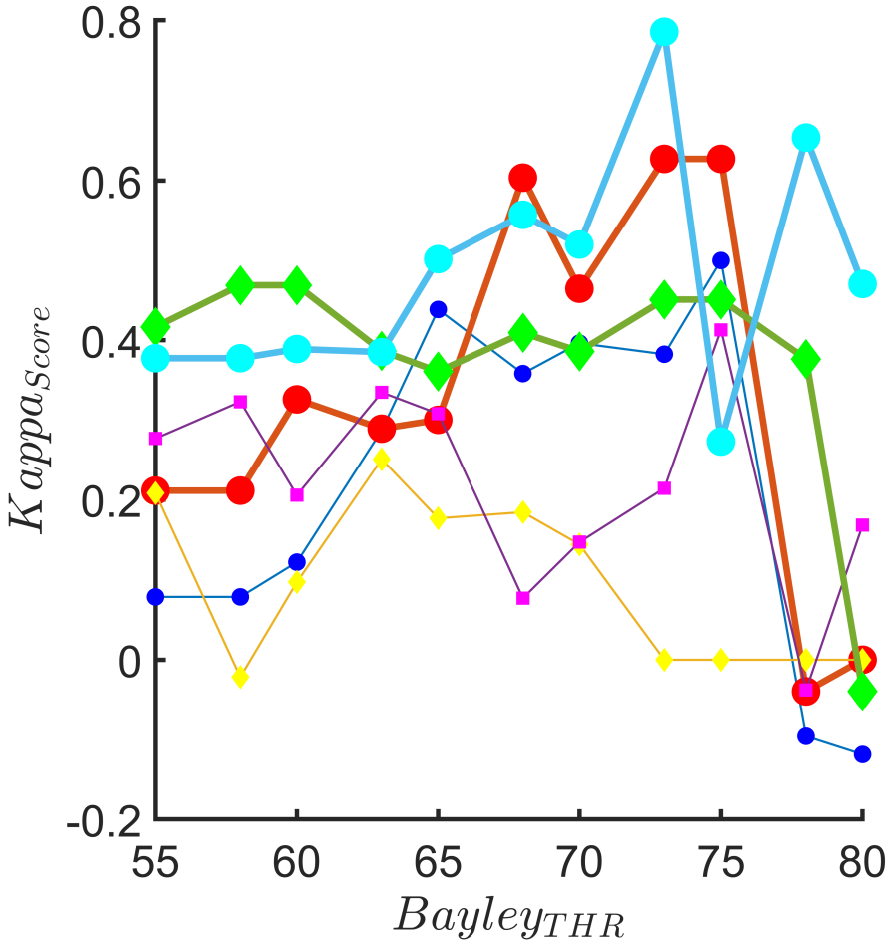
Wallois, F. (2010). Synopsis de la maturation des activités cérébrales chez le nouveau-né prématuré. *Neurophysiologie Clinique*, *40*(2), 125–126. https://doi.org/10.1016/j.neucli.2010.02.001

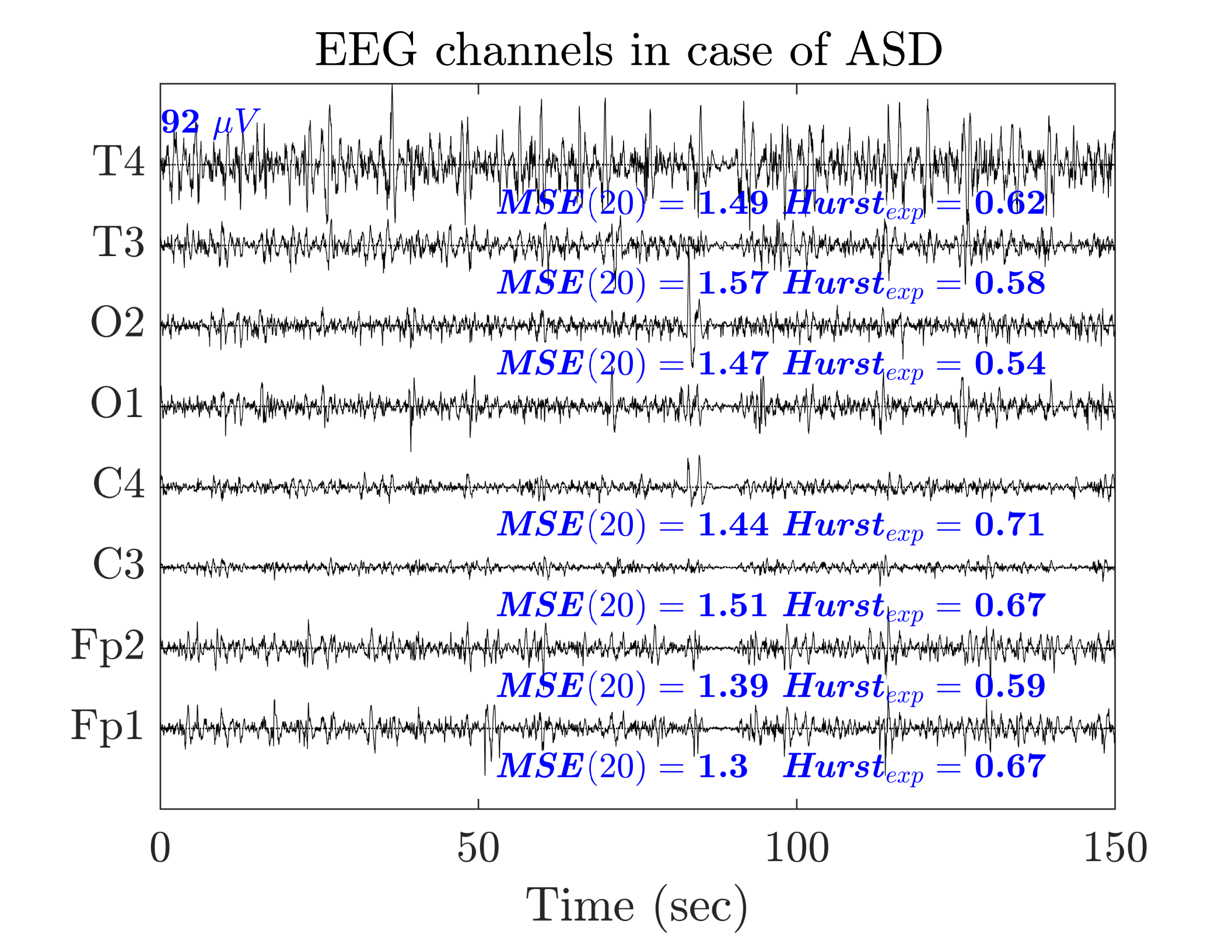
Watanabe, K., Hayakawa, F., & Okumura, A. (1999, September 1). Neonatal EEG: A powerful tool in the assessment of brain damage in preterm infants. *Brain and Development*, Vol. 21, pp. 361–372. https://doi.org/10.1016/S0387-7604(99)00034-0

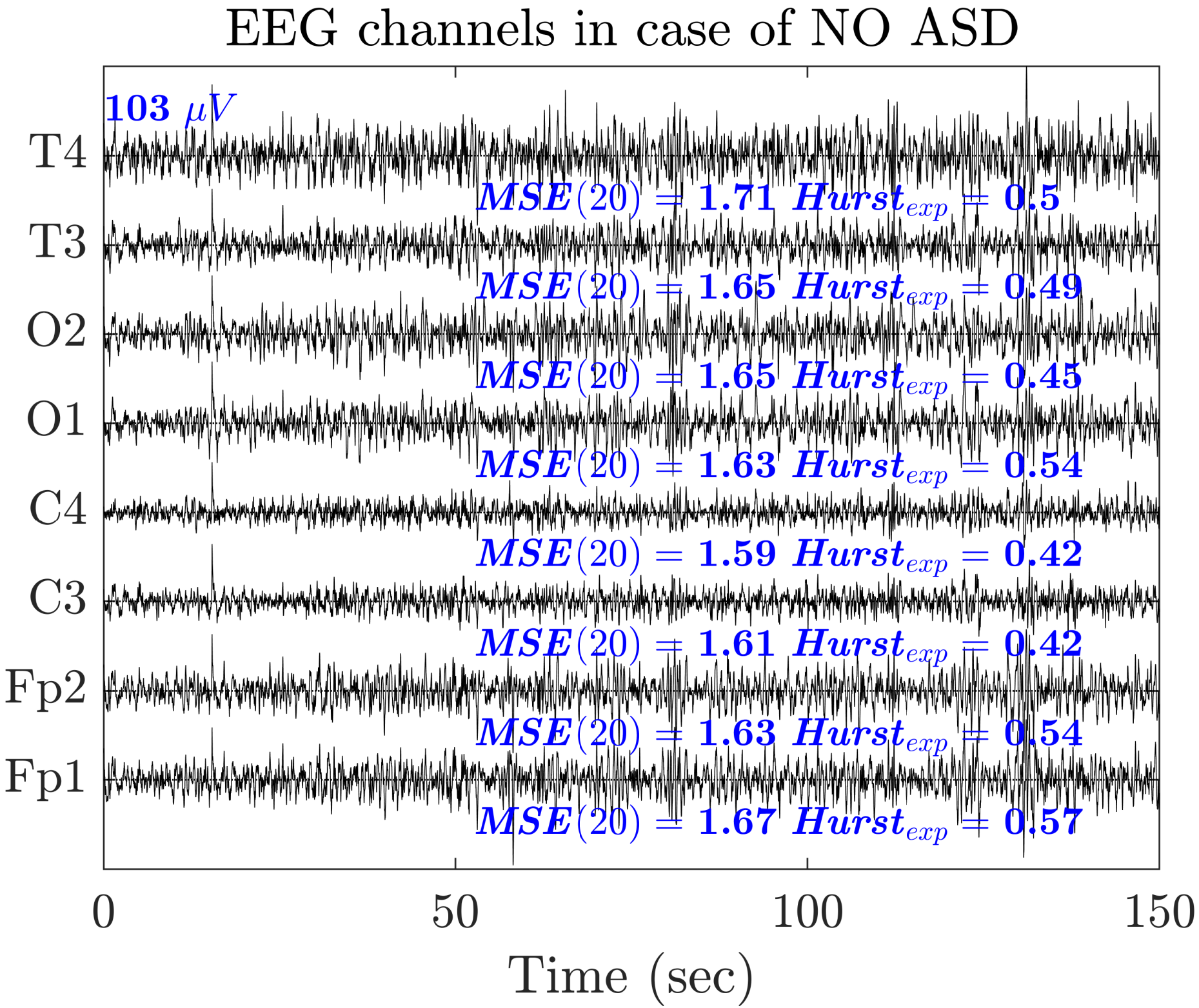
Wendt, H., Abry, P., & Jaffard, S. (2007). Bootstrap for Multifractal Analysis. *IEEE Signal Processing Magazine*, *24*(4), 38–48. https://doi.org/10.1109/MSP.2007.4286563

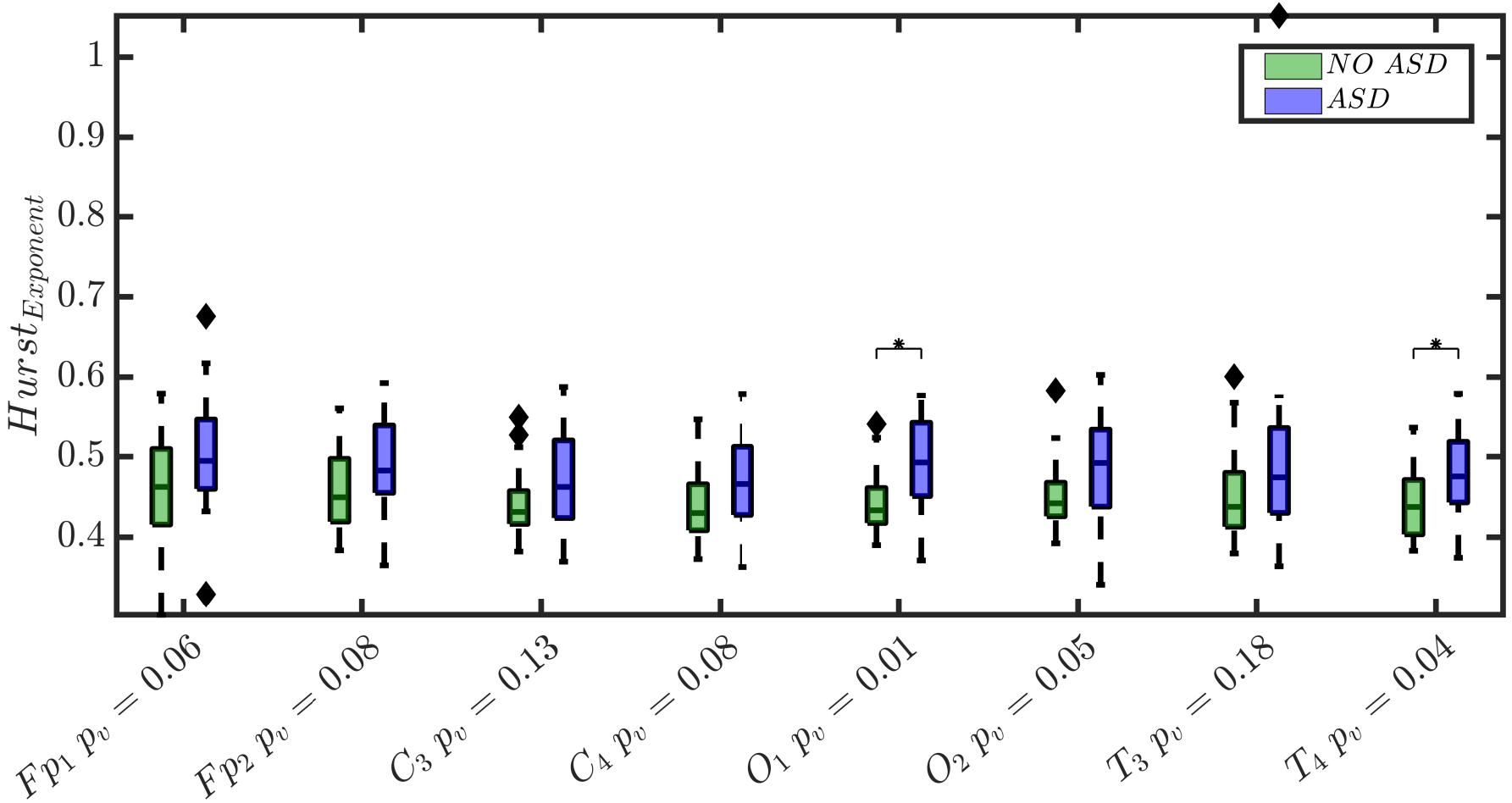
Zhang, D., Ding, H. H., Liu, Y., Zhou, C., Ding, H. H., & Ye, D. (2009). Neurodevelopment in newborns: A sample entropy analysis of electroencephalogram. *Physiological Measurement*, *30*(5), 491–504. https://doi.org/10.1088/0967-3334/30/5/006


1
0.9
0.8
0.7
0.6
0.5
0.4
0.3
0.2
AUC
55
60
65
70
75
80
Bayley_THR
Power
MSE
rEEG
Conn
MFA
All

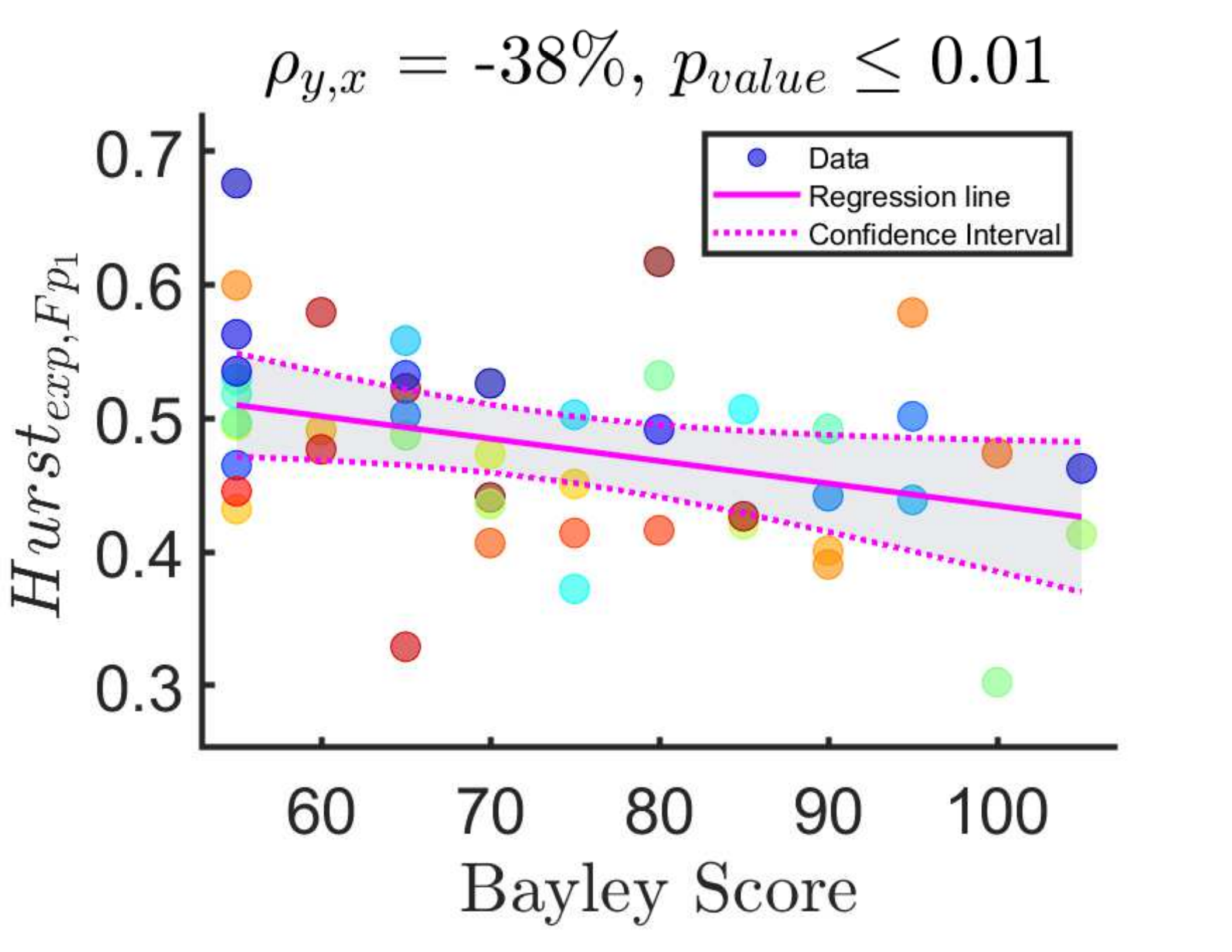

0.8
0.6
0.4
0.2
0
-0.2
Kappa_Score
55
60
65
70
75
80
Bayley_THR

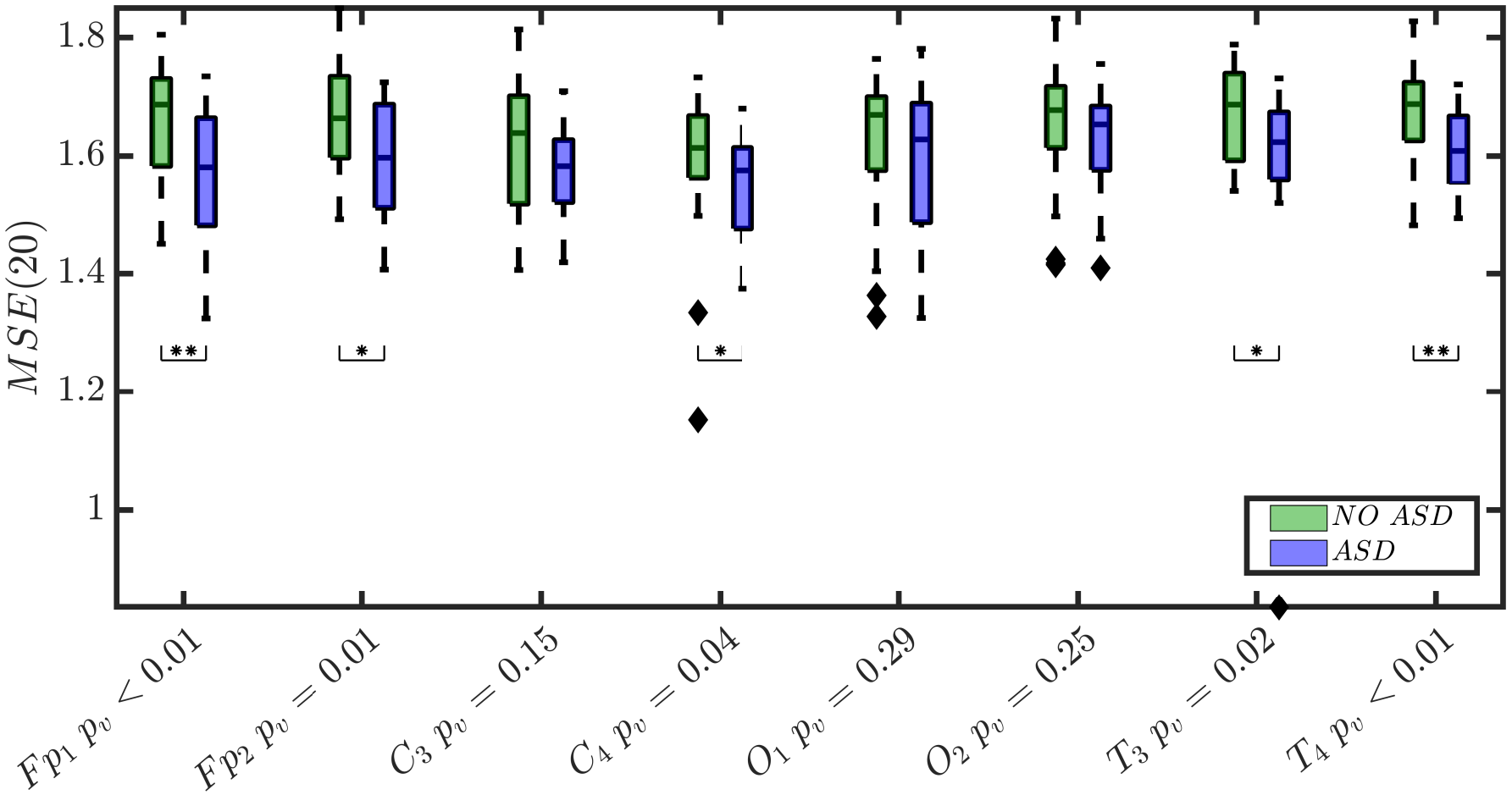

EEG channels in case of ASD
92 μV
T4
T3
O2
O1
C4
C3
Fp2
Fp1
$MSE(20) = 1.49$ $Hurst_{exp} = 0.62$
$MSE(20) = 1.57$ $Hurst_{exp} = 0.58$
$MSE(20) = 1.47$ $Hurst_{exp} = 0.54$
$MSE(20) = 1.44$ $Hurst_{exp} = 0.71$
$MSE(20) = 1.51$ $Hurst_{exp} = 0.67$
$MSE(20) = 1.39$ $Hurst_{exp} = 0.59$
$MSE(20) = 1.3$ $Hurst_{exp} = 0.67$
0
50
100
150
Time (sec)

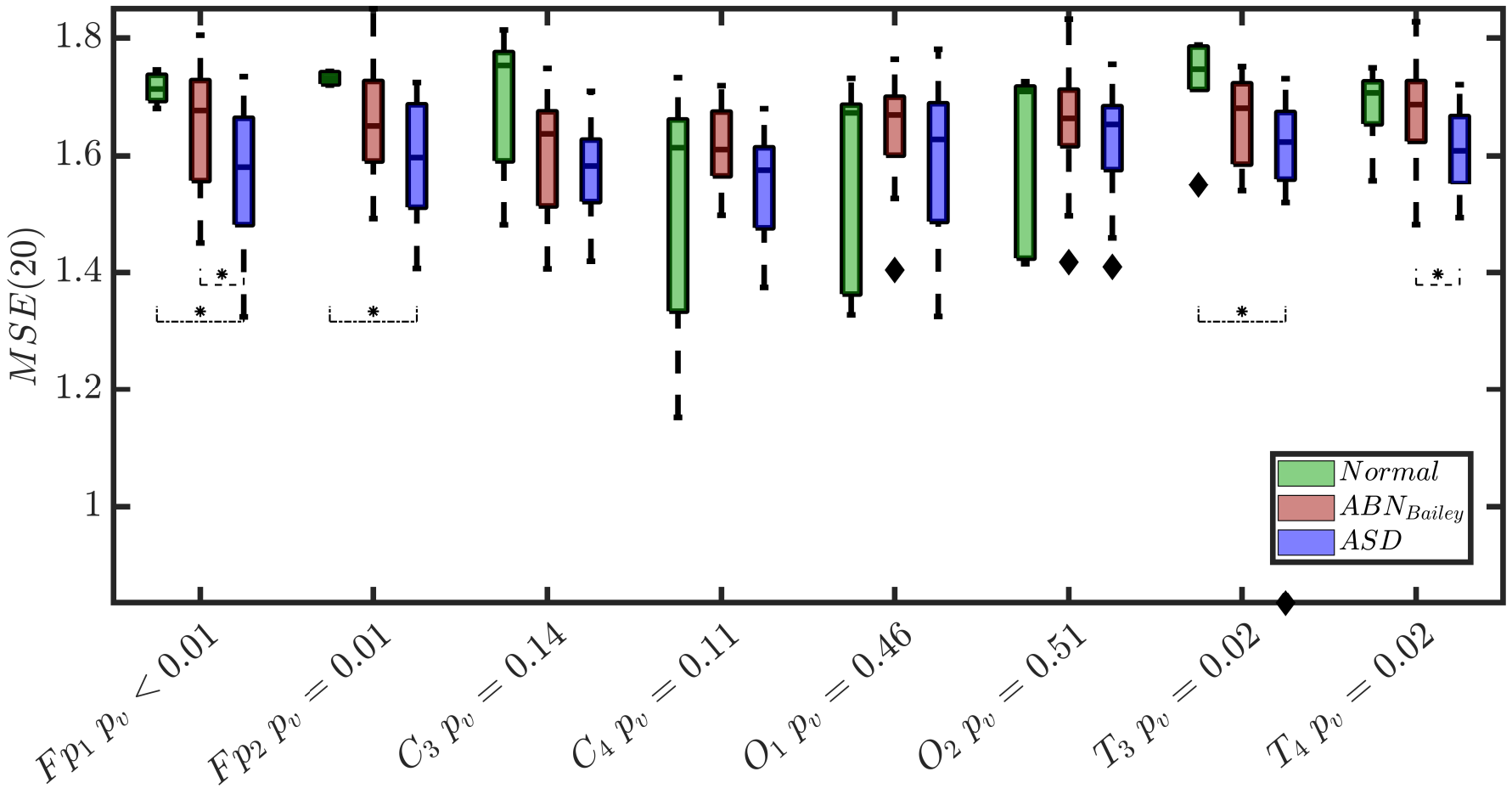

EEG channels in case of NO ASD
103 μV
T4
T3
O2
O1
C4
C3
Fp2
Fp1
MSE(20) = 1.71 Hurst_exp = 0.5
MSE(20) = 1.65 Hurst_exp = 0.49
MSE(20) = 1.65 Hurst_exp = 0.45
MSE(20) = 1.63 Hurst_exp = 0.54
MSE(20) = 1.59 Hurst_exp = 0.42
MSE(20) = 1.61 Hurst_exp = 0.42
MSE(20) = 1.63 Hurst_exp = 0.54
MSE(20) = 1.67 Hurst_exp = 0.57
0
50
100
150
Time (sec)

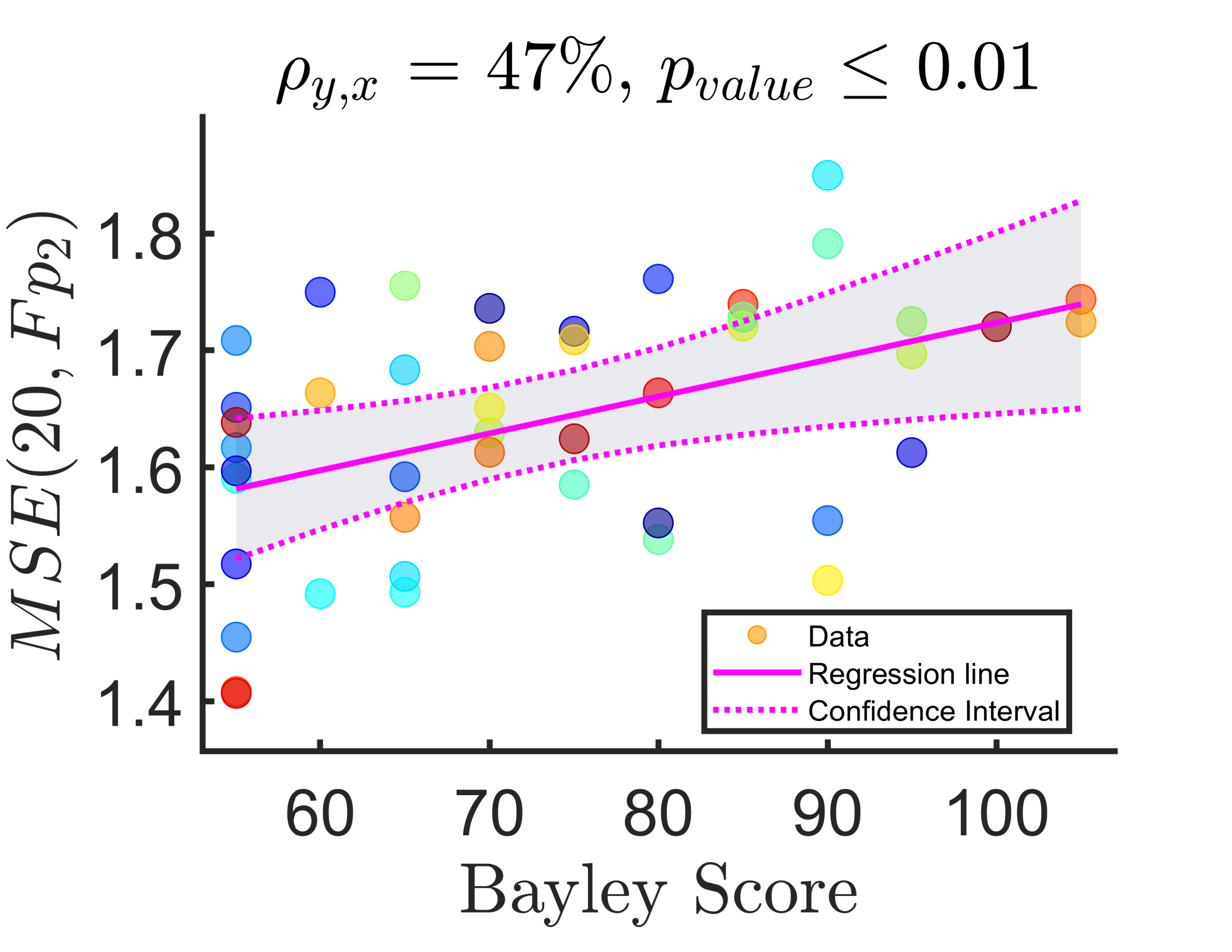

NO ASD
ASD
$Hurst_{Exponent}$
1
0.9
0.8
0.7
0.6
0.5
0.4
*
*
$Fp_1\ p_v = 0.06$
$Fp_2\ p_v = 0.08$
$C_3\ p_v = 0.13$
$C_4\ p_v = 0.08$
$O_1\ p_v = 0.01$
$O_2\ p_v = 0.05$
$T_3\ p_v = 0.18$
$T_4\ p_v = 0.04$

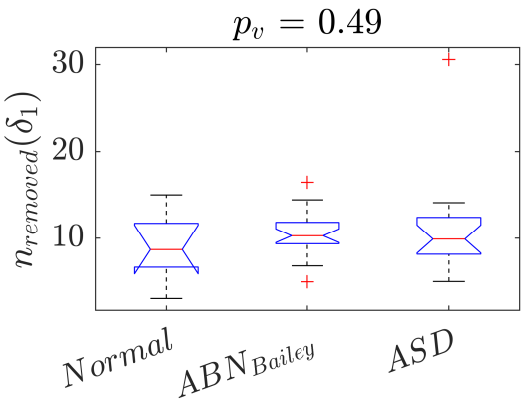
Normal
ABN_Bailey
ASD
Hurst Exponent
1
0.9
0.8
0.7
0.6
0.5
0.4
Fp1 p_v = 0.12
Fp2 p_v = 0.21
C3 p_v = 0.32
C4 p_v = 0.17
O1 p_v = 0.03
O2 p_v = 0.05
T3 p_v = 0.37
T4 p_v = 0.1

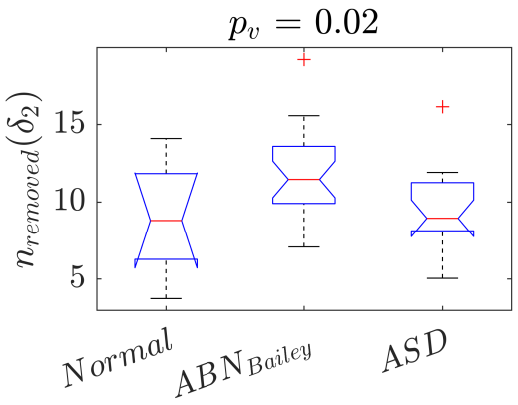

$\rho_{y,x} = -38\%,\ p_{value} \leq 0.01$
Data
Regression line
Confidence Interval
$Hurst_{exp,FP_1}$
0.7
0.6
0.5
0.4
0.3
60
70
80
90
100
Bayley Score

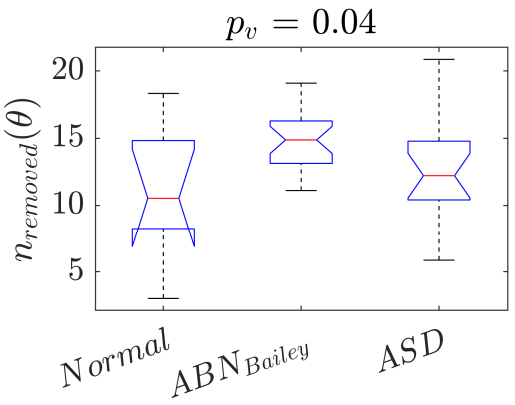

MSE(20)
1.8
1.6
1.4
1.2
1
**
*
*
*
**
NO ASD
ASD
Fp1 pv < 0.01
Fp2 pv = 0.01
C3 pv = 0.15
C4 pv = 0.04
O1 pv = 0.29
O2 pv = 0.25
T3 pv = 0.02
T4 pv < 0.01

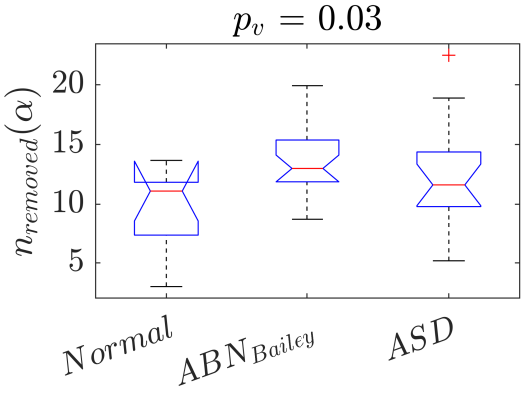

1.8
1.6
1.4
1.2
1
$MSE(20)$
*
*
*
*
*
$Normal$
ABN_{Bailey}
ASD
$Fp_1\ p_v < 0.01$
$Fp_2\ p_v = 0.01$
$C_3\ p_v = 0.14$
$C_4\ p_v = 0.11$
$O_1\ p_v = 0.46$
$O_2\ p_v = 0.51$
$T_3\ p_v = 0.02$
$T_4\ p_v = 0.02$

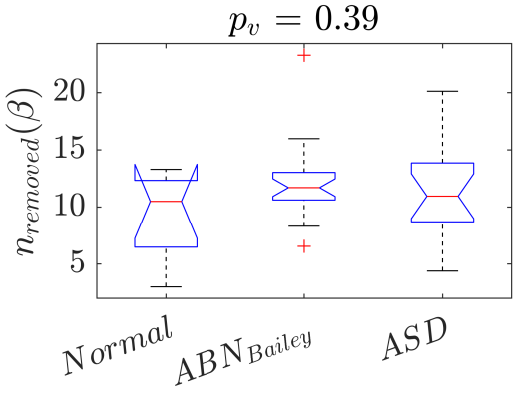

$\rho_{y,x} = 47\%,\ p_{value} \leq 0.01$
$MSE(20, Fp_2)$
1.8
1.7
1.6
1.5
1.4
60
70
80
90
100
Bayley Score
Data
Regression line
Confidence Interval


$p_v = 0.49$
$n_{removed}(\delta_1)$
30
20
10
Normal
ABN Bailey
ASD

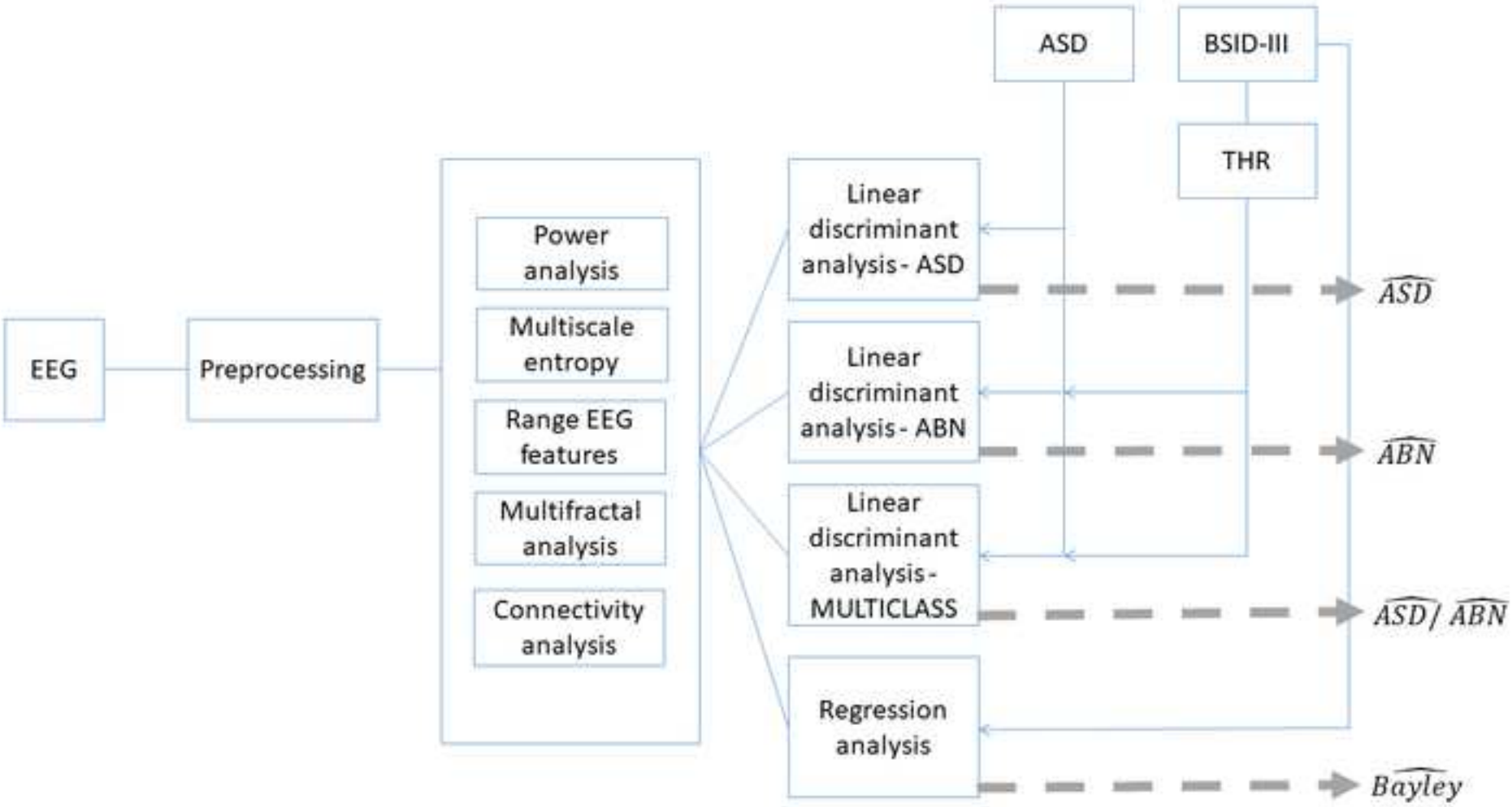

$p_v = 0.02$
$n_{removed}(\delta_2)$
15
10
5
Normal
ABN Bailey
ASD


$p_v = 0.04$
$n_{removed}(\theta)$
20
15
10
5
Normal
ABN Bailey
ASD


$p_v = 0.03$
$n_{removed}(\alpha)$
20
15
10
5
Normal
ABN Bailey
ASD


$p_v = 0.39$
$n_{removed}(\beta)$
20
15
10
5
Normal
ABN Bailey
ASD

Click here to access/download;Figure;scheme_EEG_figure_1.tif



Figure

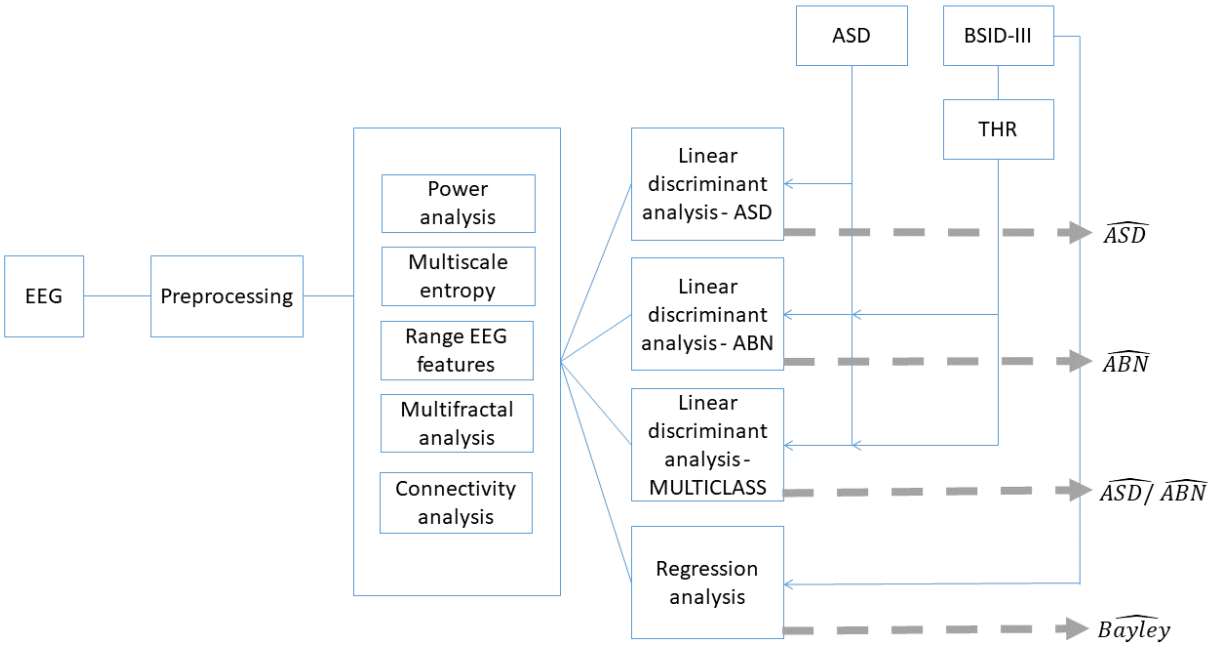


Figure 1. A schematic overview of the four strategies implemented in this study. The BSID-III stands for the Bayley Developmental Scale, ASD is autism spectrum disorder and THR is the threshold applied to define an abnormal Bayley outcome. After EEG preprocessing, a set of power, entropy, fractality, range EEG and connectivity features are derived to quantify the level of EEG dysmaturity. Those features are fed in different supervised discrimination strategies: 1) binary classification for ASD diagnosis with linear discriminant analysis (LDA), 2) binary classification with LDA for development abnormality diagnosis (ABN), 3) multiclass classification with LDA to determine if infants have ASD or if infants have only an abnormal BSID-III, 4) Regression analysis to extrapolate the Bayley score. The four supervised strategy blocks are fed with both features and the ground truth labels ASD, BSID-III (blue thin lines, BSID-III after threshold THR or the actual continuous variable for the regression analysis) and they have the prediction of ASD or abnormal outcome (dashed grey lines).

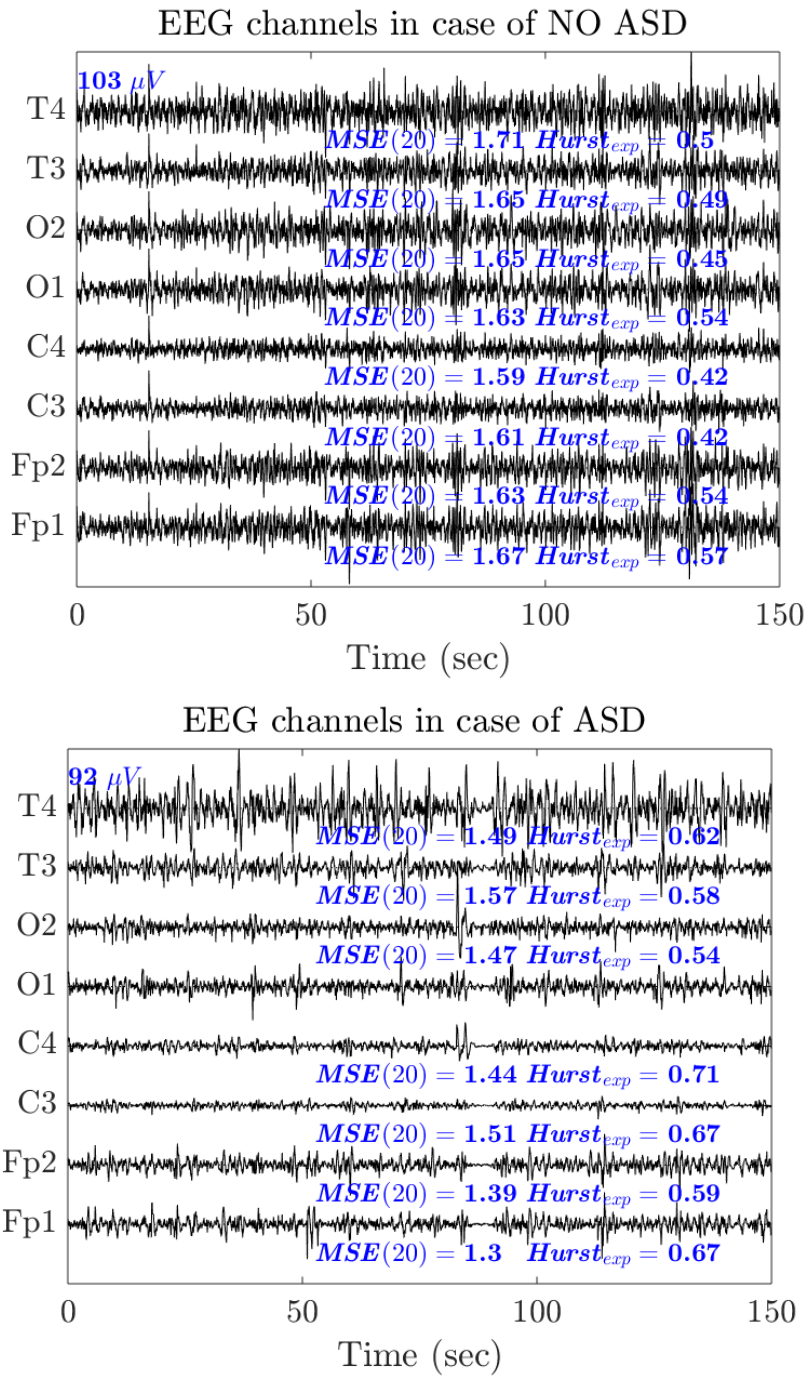


Figure 2. The figure shows two examples of EEG channels from the no ASD group (NO ASD, upper panel) and the autism spectrum disorder (ASD) group (lower panel). The data from the 8 channels are reported in a window of 150 sec and the associated entropy at scale 20 MSE(20) and the Hurst exponent are displayed if and only if the threshold criteria discussed in the text are met. The ASD EEG has lower entropy and higher Hurst exponent, which leads to a more discontinuous channel with slower rhythms. On the contrary, the EEG of a patient without ASD has faster frequencies and higher entropy at larger scale. Therefore, the ASD EEG can be considered a dysmature EEG. The sensitivity of the plotting is reported on the top left of the chart.

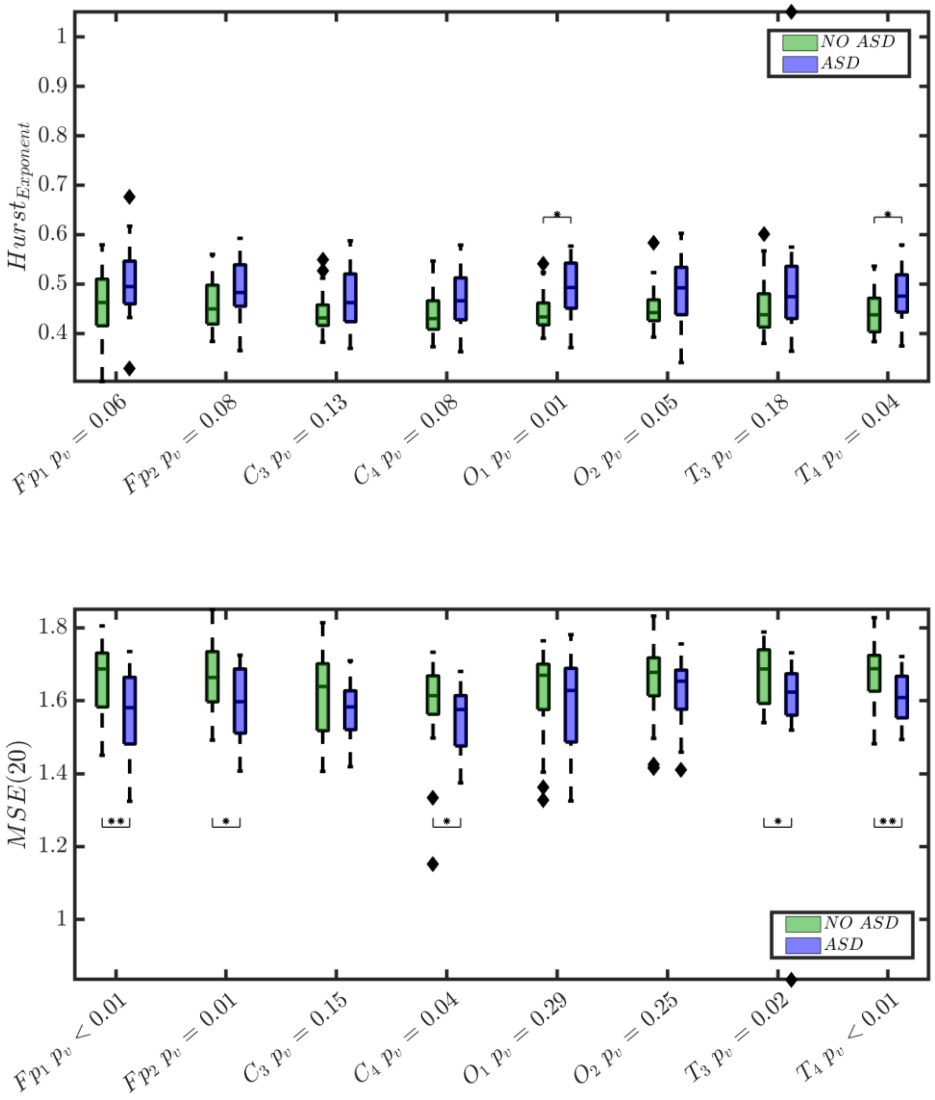


Figure 3. The figure shows the entropy at scale 20 MSE(20) and the Hurst exponent in the two groups (NO ASD = No ASD, ASD = Autism Spectrum Disorder). Both describe the persistence of slow-waves and discontinuity. In the case of ASD, the EEG presents a dysmature or disorganized pattern, since the regularity of the signal is higher due to spikiness, lack of smoothness and general discontinuity. The enhanced and abnormal slow-wave information in the disorganized EEG lowers the entropy at lower frequencies (MSE(20)). P-values have been derived with Kruskal-Wallis test. The symbols * and ** respectively represent post-hoc comparison with p-value <= 0.05 and <=0.01.

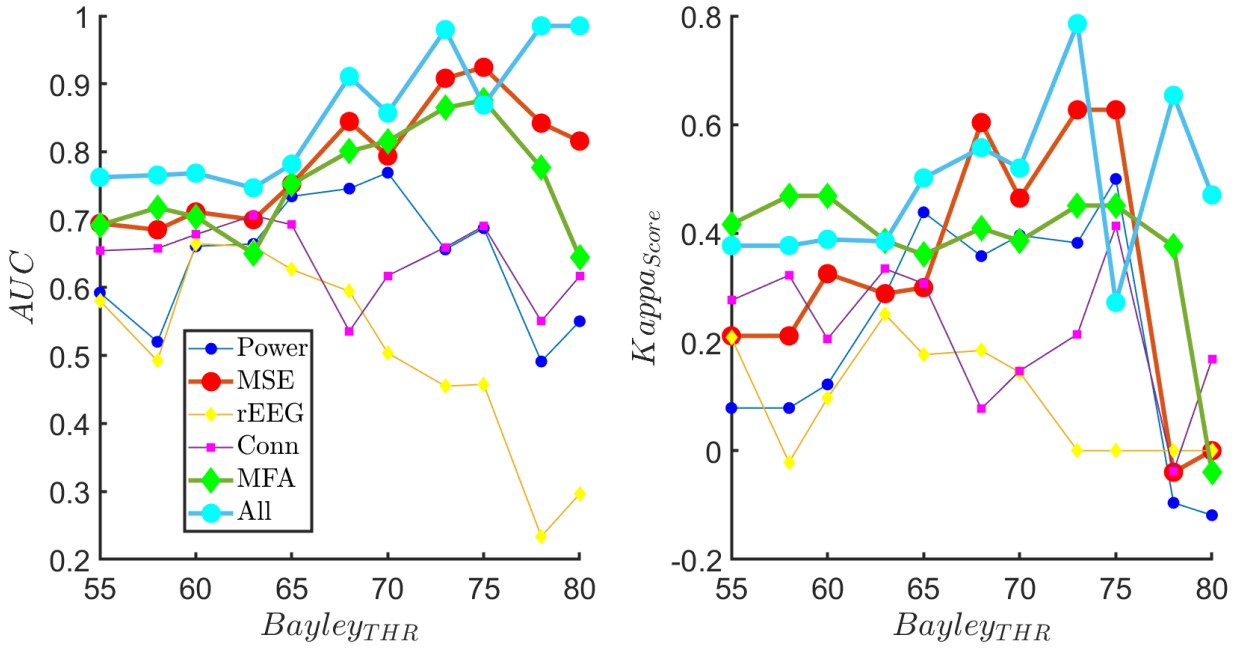


Figure 4. Binary classification performance in function of the threshold applied to BSID-III (BayleyTHR) to define the positive class. The two panels report the *linear discriminant analysis* area under the ROC curve (AUC) and Kappa score for the classification of the normal vs abnormal development group for each group of features. The abnormal group contains at least one developmental problem (ASD or abnormal Bayley). The Bayley Threshold has been used to define the abnormal Bayley outcome for each of the three investigated scores (cognitive, motor and language outcome). The reported groups of features are power, entropy (MSE), range-EEG or NEURAL features (rEEG), connectivity (Conn), fractality (MFA) and all the features combined (All). Each AUC and Kappa score chart is reported in different colors and different symbols for each feature group.

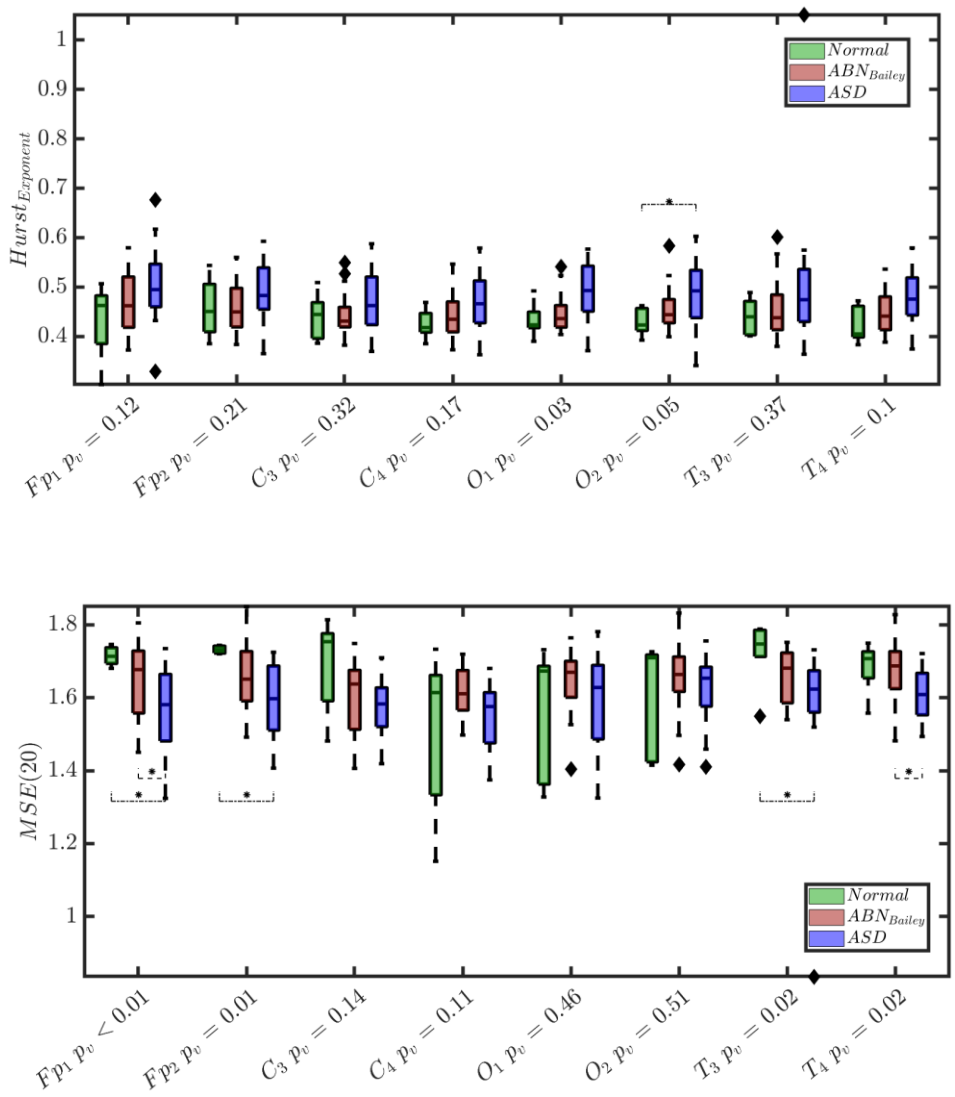


Figure 5. The figure shows the entropy at scale 20 MSE(20) and the Hurst exponent in the three groups (Normal = Normal Development, ABN-Bayley = only abnormal Bayley outcome , ASD = ASD patients). Both describe the presence of slow-waves persistence and discontinuity. The combination of ASD and abnormal development shows a more severe increase of regularity compared to other groups (especially, in the occipital area) and a more severe decrease of entropy compared to other groups (especially, in the frontal area). P-values have been derived with Kruskal-Wallis test. The symbols * and ** respectively represent post-hoc comparison with p-value <= 0.05 and <=0.01.

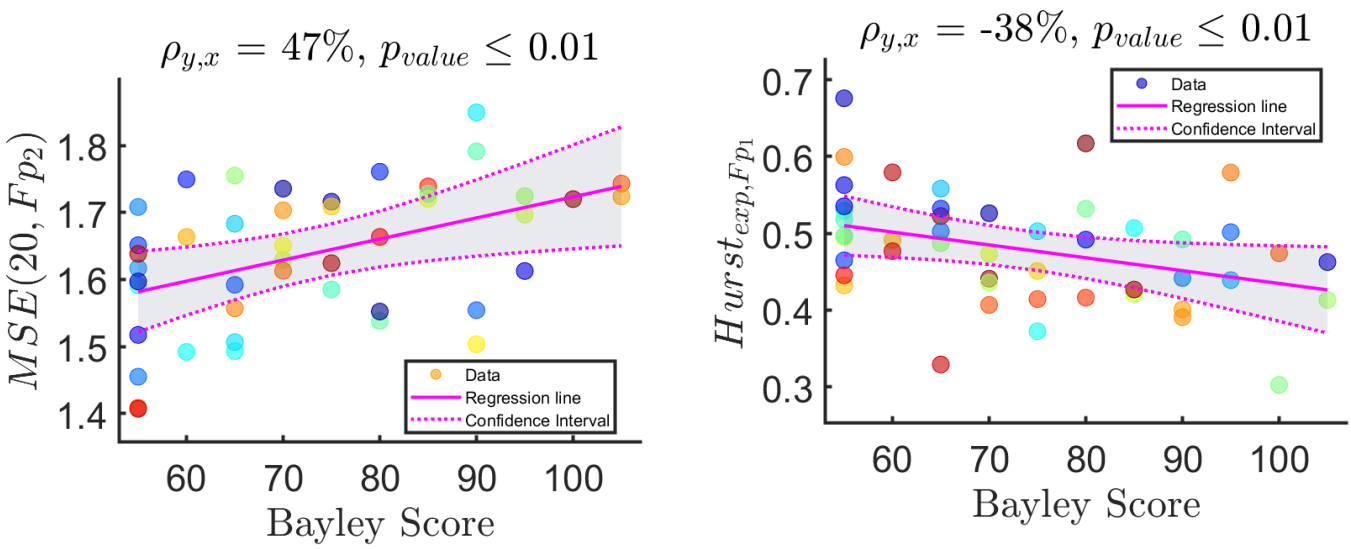


Figure 6. The figure shows the entropy at scale 20 MSE(20) and the Hurst exponent in function of the Cognitive BSID-III score. The two panels reported the cluster of data points (circles with a color for each patient), the expected value of the considered feature for each Bayley score (pink thick line) and the 95% confidence intervals (pink dashed lines). The left panel clearly shows that the higher the Bayley score the higher the entropy at scale 20, while the right panel shows that the higher the cognitive score the lower the Hurst exponent. The figure confirms that both entropy and the regularity are features of brain dysmaturity, and are related to developmental outcome in ASD subjects. In addition, the increase of MSE(20) underlines how the persistence of slow-waves is related to a worse developmental outcome.

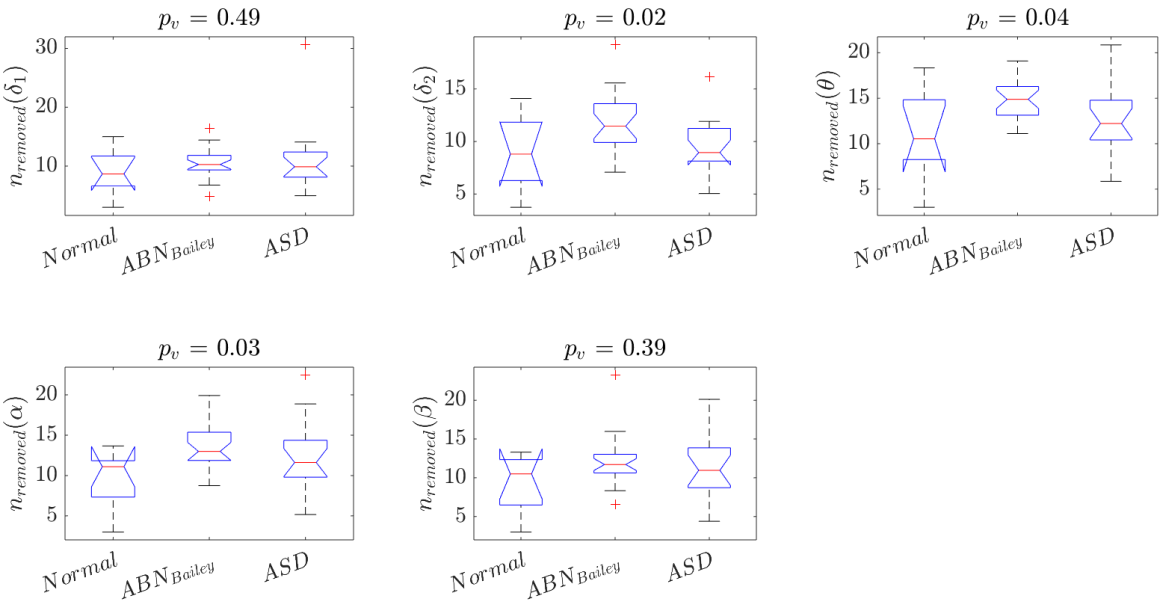


Figure 7. The measure of network redundancy is shown for the three different study groups: normal, abnormal Bayley outcome (Bayley < 80) and ASD with an abnormal Bayley. As shown by the second and third panel, the number of superfluous connections (nsup or Nremoved) is higher in case of development abnormalities.

Table

Click here to access/download
Table
QEEG_analysis_epistop_tables_CMPB_2020_09_14.docx

Results of quantitative EEG analysis are associated with autism spectrum disorder and development abnormalities in infants with tuberous sclerosis complex

Mario Lavanga[1], Jessie De Ridder[2], Katarzyna Kotulska[3], Romina Moavero[4,5], Paolo Curatolo[4], Bernhard Weschke[6], Kate Riney[7,8], Martha Feucht[9], Pavel Krsek[10], Rima Nabbout[11], Anna C. Jansen[12], Konrad Wojdan[13,14], Dorota Domanska-Pakieła[3], Magdalena Kaczorowska-Frontczak[3], Christoph Hertzberg[15], Cyrille H. Ferrier[16], Sharon Samueli[9], Alena Jahodova[10], Eleonora Aronica[17], David J. Kwiatkowski[19], Floor E. Jansen[16], Sergiusz Jóźwiak[3,20], Lieven Lagae[2], Sabine Van Huffel[1], Alexander Caicedo[21] on behalf of the EPISTOP consortium

Conflict of interest statement

The authors declare that the research was conducted in the absence of any commercial or financial relationships that could be construed as a potential conflict of interest.